



THE UNIVERSITY *of* EDINBURGH

Edinburgh Research Explorer

## Assessment of left atrial volume in dogs

**Citation for published version:**

Bouvard, J, Thierry, F, Culshaw, G, Schwarz, T, Handel, I & Martinez-Pereira, Y 2019, 'Assessment of left atrial volume in dogs: comparisons of two-dimensional and real-time three-dimensional echocardiography with ECG-gated multidetector computed tomography angiography', *Journal of Veterinary Cardiology*.  
<https://doi.org/10.1016/j.jvc.2019.06.004>

**Digital Object Identifier (DOI):**

[10.1016/j.jvc.2019.06.004](https://doi.org/10.1016/j.jvc.2019.06.004)

**Link:**

[Link to publication record in Edinburgh Research Explorer](#)

**Document Version:**

Peer reviewed version

**Published In:**

Journal of Veterinary Cardiology

**General rights**

Copyright for the publications made accessible via the Edinburgh Research Explorer is retained by the author(s) and / or other copyright owners and it is a condition of accessing these publications that users recognise and abide by the legal requirements associated with these rights.

**Take down policy**

The University of Edinburgh has made every reasonable effort to ensure that Edinburgh Research Explorer content complies with UK legislation. If you believe that the public display of this file breaches copyright please contact [openaccess@ed.ac.uk](mailto:openaccess@ed.ac.uk) providing details, and we will remove access to the work immediately and investigate your claim.



## Manuscript Details

<b>Manuscript number</b>	JVC_2018_115_R4
<b>Title</b>	Assessment of left atrial volume in dogs: comparisons of two-dimensional and real-time three-dimensional echocardiography with ECG-gated multidetector computed tomography angiography.
<b>Article type</b>	Clinical Studies

### Abstract

Introduction: We hypothesised that real-time three-dimensional echocardiography (RT-3DE) was superior to bi-dimensional (2D) echocardiography for the estimation of left atrial volume (LAV), using electrocardiographic (ECG)-gated multidetector computed tomography angiography (MDCTA) as a volumetric gold standard. The aim was to compare maximum LAV (LAVmax) and minimum LAV (LAVmin) measured by biplane area-length method (ALM), biplane method of disk (MOD) and RT-3DE with 64-slice ECG-gated MDCTA in dogs. Animals: Twenty dogs, anaesthetised for various diagnostic purposes and without evidence of cardiovascular disease. Methods: Left atrial volume was estimated by ALM, MOD and RT-3DE following ECG-gated MDCTA. The results were compared with LAV from MDCTA and correlations were performed. The limits of agreement (LoA) between methods were evaluated using Bland-Altman analysis and intra class correlations. Coefficients of variation were calculated. Results: Area-length method ( $r = 0.79$  and  $0.72$ ), MOD ( $r = 0.81$  and  $0.70$ ) and RT-3DE ( $r = 0.94$  and  $0.82$ ) correlated with MDCTA for LAVmax and LAVmin respectively (all  $p < 0.05$ ). Biases for LAVmax ( $-0.96$  mL, 95% LoA:  $-5.6 - 3.7$ ) and LAVmin ( $-0.67$  mL, 95% LoA:  $-5.4 - 4.1$ ) were minimal with RT-3DE, reflecting a slight underestimation. Conversely, MOD (LAVmaxbias =  $3.19$  mL, 95% LoA:  $-5.7 - 12.1$ ; LAVminbias =  $1.96$  mL, 95% LoA:  $-4.6 - 8.5$ ) and ALM (LAVmaxbias =  $4.05$ , 95% LoA:  $-5.7 - 13.8$ ; LAVminbias =  $2.80$  mL, 95% LoA:  $-3.9 - 9.5$ ) suggested LAV overestimation. Intra- and inter-observer variability were adequate. Conclusions: Real-time three-dimensional echocardiography is a non-invasive, accurate and feasible method with superior accuracy to 2D methods.

<b>Keywords</b>	canine; cardiac volumes; biplane modified Simpson method; biplane area-length method; advanced cardiac imaging
<b>Corresponding Author</b>	Jonathan Bouvard
<b>Corresponding Author's Institution</b>	University of Edinburgh
<b>Order of Authors</b>	Jonathan Bouvard, Florence Thierry, Geoff Culshaw, Tobias Schwarz, Ian Handel, Yolanda Martinez Pereira

## Submission Files Included in this PDF

### File Name [File Type]

Letter to editor reply 4.docx [Response to Reviewers]

Abstract and keywords-review2Cor.docx [Abstract]

Title page-review2.docx [Title Page (with Author Details)]

Manuscript-reviewEditors-Cor Biblio.docx [Manuscript File]

Figure 1.tiff [Figure]

Figure 2.tiff [Figure]

Figure 3.tiff [Figure]

Figure 4review2.tiff [Figure]

Figure 5.tiff [Figure]

References supplementary table-review2Cor.docx [Table]

Supplementary table-review2Cor.docx [Table]

Table 1-review2Cor.docx [Table]

Table 2-review2Cor.docx [Table]

Table 3-review2Cor.docx [Table]

Author Form JVC.docx [Author Agreement]

## Submission Files Not Included in this PDF

### File Name [File Type]

Video I Left atrial volume RT-3DE.avi [Video]

To view all the submission files, including those not included in the PDF, click on the manuscript title on your EVISE Homepage, then click 'Download zip file'.

## Research Data Related to this Submission

There are no linked research data sets for this submission. The following reason is given:  
Data will be made available on request



The Hospital for Small Animals  
Royal (Dick) School of Veterinary Studies  
Easter Bush Campus  
Midlothian  
EH25 9RG

2<sup>nd</sup> June 2019

Dear Dr Fonfara,  
Editor-in-Chief  
Journal of Veterinary Cardiology

Re: Invitation to revise manuscript JVC\_2018\_115, Assessment of left atrial volume in dogs: comparisons of two-dimensional and real-time three-dimensional echocardiography with ECG-gated multidetector computed tomography angiography.

Thank you again for conditionally accepting our manuscript.  
My apologies for the missed editorial changes. I reviewed the complete manuscript and have had it proof read by a colleague before resubmission. I hope that it will be satisfactory to process the manuscript further.

Thank you very much for your kind feedback and your consideration of this resubmitted manuscript.

Yours sincerely,

Dr. Jonathan Bouvard



1  
2  
3 **Abstract**  
4

5 **Introduction:** We hypothesised that real-time three-dimensional echocardiography  
6 (RT-3DE) was superior to bi-dimensional (2D) echocardiography for the estimation of  
7 left atrial volume (LAV), using electrocardiographic (ECG)-gated multidetector  
8 computed tomography angiography (MDCTA) as a volumetric gold standard. The aim  
9 was to compare maximum LAV ( $LAV_{max}$ ) and minimum LAV ( $LAV_{min}$ ) measured by  
10 biplane area-length method (ALM), biplane method of disk (MOD) and RT-3DE with  
11 64-slice ECG-gated MDCTA in dogs.

12 **Animals:** Twenty dogs, anaesthetised for various diagnostic purposes and without  
13 evidence of cardiovascular disease.

14 **Methods:** Left atrial volume was estimated by ALM, MOD and RT-3DE following ECG-  
15 gated MDCTA. The results were compared with LAV from MDCTA and correlations  
16 were performed. The limits of agreement (LoA) between methods were evaluated  
17 using Bland-Altman analysis and intra class correlations. Coefficients of variation were  
18 calculated.

19 **Results:** Area-length method ( $r = 0.79$  and  $0.72$ ), MOD ( $r = 0.81$  and  $0.70$ ) and RT-  
20 3DE ( $r = 0.94$  and  $0.82$ ) correlated with MDCTA for  $LAV_{max}$  and  $LAV_{min}$  respectively (all  
21  $p < 0.05$ ). Biases for  $LAV_{max}$  ( $-0.96$  mL, 95% LoA:  $-5.6 - 3.7$ ) and  $LAV_{min}$  ( $-0.67$  mL, 95%  
22 LoA:  $-5.4 - 4.1$ ) were minimal with RT-3DE, reflecting a slight underestimation.  
23 Conversely, MOD ( $LAV_{max}$  bias =  $3.19$  mL, 95% LoA:  $-5.7 - 12.1$ ;  $LAV_{min}$  bias =  $1.96$   
24 mL, 95% LoA:  $-4.6 - 8.5$ ) and ALM ( $LAV_{max}$  bias =  $4.05$ , 95% LoA:  $-5.7 - 13.8$ ;  
25  $LAV_{min}$  bias =  $2.80$  mL, 95% LoA:  $-3.9 - 9.5$ ) suggested LAV overestimation. Intra- and  
inter-observer variability were adequate.

26 **Conclusions:** Real-time three-dimensional echocardiography is a non-invasive,  
27 accurate and feasible method with superior accuracy to 2D methods.  
28  
29  
30  
31  
32  
33  
34  
35  
36  
37  
38  
39  
40  
41  
42  
43  
44  
45  
46  
47  
48  
49  
50  
51

60  
61  
62  
63  
64  
65  
66  
67  
68  
69  
70  
71  
72  
73  
74  
75  
76  
77  
78  
79  
80  
81  
82  
83  
84  
85  
86  
87  
88  
89  
90  
91  
92  
93  
94  
95  
96  
97  
98  
99  
100  
101  
102  
103  
104  
105  
106  
107  
108  
109  
110  
111  
112  
113  
114  
115  
116  
117  
118

26

27 **Key words:** canine; cardiac volumes; biplane modified Simpson method; biplane area-

28 length method; advanced cardiac imaging

29

1  
2  
3 **1 Assessment of left atrial volume in dogs: comparisons of two-dimensional and**  
4 **2 real-time three-dimensional echocardiography with ECG-gated multidetector**  
5 **3 computed tomography angiography**

6  
7  
8  
9  
10 **4 Short title: Two-dimensional and three-dimensional estimations of left atrial**  
11 **5 volume in dogs**

12  
13  
14  
15  
16 Jonathan Bouvard (<https://orcid.org/0000-0002-1540-3860>), DVM, Florence Thierry  
17  
18 (<https://orcid.org/0000-0003-4175-4397>), DVM, Geoffrey J. Culshaw ([https://orcid.org/0000-](https://orcid.org/0000-0003-2400-6178)  
19 [0003-2400-6178](https://orcid.org/0003-2400-6178)), BVMS, PhD, Tobias Schwarz (<https://orcid.org/0000-0001-8412-573X>),  
20  
21 DVM, Ian Handel, BVSc, MSci, PhD, Yolanda Martinez-Pereira, Lda Vet.  
22  
23  
24

25  
26  
27 The Royal (Dick) School of Veterinary Studies, Division of Clinical Veterinary Sciences,  
28  
29 University of Edinburgh, Edinburgh, UK.  
30  
31

32  
33 Corresponding author: Jonathan Bouvard

34  
35 ORCID number: <https://orcid.org/0000-0002-1540-3860>

36  
37 E-mail address: [j.bouvard@ed.ac.uk](mailto:j.bouvard@ed.ac.uk)  
38  
39

40  
41  
42 Results were presented at the 28<sup>th</sup> congress of the European College of Veterinary  
43  
44 Internal Medicine Companion Animals, Rotterdam, Netherlands, 2018.  
45  
46  
47  
48  
49  
50  
51  
52  
53  
54  
55  
56  
57  
58  
59

1  
2  
3 **1 Assessment of left atrial volume in dogs: comparisons of two-dimensional and**  
4 **2 real-time three-dimensional echocardiography with ECG-gated multidetector**  
5 **3 computed tomography angiography**

6  
7  
8  
9  
10 **4 Short title: Two-dimensional and three-dimensional estimations of left atrial**  
11 **5 volume in dogs**

12  
13  
14  
15  
16 Jonathan Bouvard (<https://orcid.org/0000-0002-1540-3860>), DVM, Florence Thierry  
17  
18 (<https://orcid.org/0000-0003-4175-4397>), DVM, Geoffrey J. Culshaw ([https://orcid.org/0000-](https://orcid.org/0000-0003-2400-6178)  
19 [0003-2400-6178](https://orcid.org/0003-2400-6178)), BVMS, PhD, Tobias Schwarz (<https://orcid.org/0000-0001-8412-573X>),  
20  
21  
22 DVM, Ian Handel, BVSc, MSci, PhD, Yolanda Martinez-Pereira, Lda Vet.

23  
24  
25  
26  
27 The Royal (Dick) School of Veterinary Studies, Division of Clinical Veterinary Sciences,  
28  
29 University of Edinburgh, Edinburgh, UK.

30  
31  
32  
33 Corresponding author: Jonathan Bouvard

34  
35 ORCID number: <https://orcid.org/0000-0002-1540-3860>

36  
37 E-mail address: [j.bouvard@ed.ac.uk](mailto:j.bouvard@ed.ac.uk)

38  
39  
40  
41  
42 Results were presented at the 28<sup>th</sup> congress of the European College of Veterinary  
43  
44 Internal Medicine Companion Animals, Rotterdam, Netherlands, 2018.

60  
61  
62 **Abstract**  
63

64 **Introduction:** We hypothesised that real-time three-dimensional echocardiography  
65 (RT-3DE) was superior to bi-dimensional (2D) echocardiography for the estimation of  
66 left atrial volume (LAV), using electrocardiographic (ECG)-gated multidetector  
67 computed tomography angiography (MDCTA) as a volumetric gold standard. The aim  
68 was to compare maximum LAV ( $LAV_{max}$ ) and minimum LAV ( $LAV_{min}$ ) measured by  
69 biplane area-length method (ALM), biplane method of disk (MOD) and RT-3DE with  
70 64-slice ECG-gated MDCTA in dogs.  
71  
72

73 **Animals:** Twenty dogs, anaesthetised for various diagnostic purposes and without  
74 evidence of cardiovascular disease.  
75  
76

77 **Methods:** Left atrial volume was estimated by ALM, MOD and RT-3DE following ECG-  
78 gated MDCTA. The results were compared with LAV from MDCTA and correlations  
79 were performed. The limits of agreement (LoA) between methods were evaluated  
80 using Bland-Altman analysis and intra class correlations. Coefficients of variation were  
81 calculated.  
82  
83

84 **Results:** Area-length method ( $r = 0.79$  and  $0.72$ ), MOD ( $r = 0.81$  and  $0.70$ ) and RT-  
85 3DE ( $r = 0.94$  and  $0.82$ ) correlated with MDCTA for  $LAV_{max}$  and  $LAV_{min}$  respectively (all  
86  $p < 0.05$ ). Biases for  $LAV_{max}$  ( $-0.96$  mL, 95% LoA:  $-5.6 - 3.7$ ) and  $LAV_{min}$  ( $-0.67$  mL, 95%  
87 LoA:  $-5.4 - 4.1$ ) were minimal with RT-3DE, reflecting a slight underestimation.  
88 Conversely, MOD ( $LAV_{max}$  bias =  $3.19$  mL, 95% LoA:  $-5.7 - 12.1$ ;  $LAV_{min}$  bias =  $1.96$   
89 mL, 95% LoA:  $-4.6 - 8.5$ ) and ALM ( $LAV_{max}$  bias =  $4.05$ , 95% LoA:  $-5.7 - 13.8$ ;  
90  $LAV_{min}$  bias =  $2.80$  mL, 95% LoA:  $-3.9 - 9.5$ ) suggested LAV overestimation. Intra- and  
91 inter-observer variability were adequate.  
92  
93

94 **Conclusions:** Real-time three-dimensional echocardiography is a non-invasive,  
95 accurate and feasible method with superior accuracy to 2D methods.  
96  
97  
98  
99  
100  
101  
102  
103  
104  
105  
106  
107  
108  
109  
110  
111  
112  
113  
114  
115  
116  
117  
118

119  
120  
121  
122  
123  
124  
125  
126  
127  
128  
129  
130  
131  
132  
133  
134  
135  
136  
137  
138  
139  
140  
141  
142  
143  
144  
145  
146  
147  
148  
149  
150  
151  
152  
153  
154  
155  
156  
157  
158  
159  
160  
161  
162  
163  
164  
165  
166  
167  
168  
169  
170  
171  
172  
173  
174  
175  
176  
177

47

48 **Key words:** canine; cardiac volumes; biplane modified Simpson method; biplane area-  
49 length method; advanced cardiac imaging

50

51 **Abbreviations**

2D	two-dimensional
3D	three-dimensional
ALM	area-length method
CI	confidence intervals
ECG	electrocardiographic
ICC	intraclass correlation coefficient
LA	left atrium
LAV	left atrial volume
LAV <sub>max</sub>	maximum left atrial volume
LAV <sub>min</sub>	minimum left atrial volume
LoA	limits of agreement
MDCTA	multi-detector computed tomography angiography
MOD	method of disk
RT-3DE	real-time three-dimensional echocardiography

52

53

178  
179  
180 **54 Introduction**  
181

182 55 Left atrial size is a clinically useful measurement in left-sided cardiac disease, and is  
183 56 acknowledged as a predictor of morbidity and mortality in human and veterinary  
184 57 medicine [1–5]. Left atrial size is routinely measured clinically with two-dimensional  
185 58 (2D) transthoracic echocardiography at ventricular end-systole or early diastole, and  
186 59 indexed to aortic root (short axis) [6–8]. However, the left atrium (LA) is a three-  
187 60 dimensional (3D) structure with complex geometry, and because LA enlargement may  
188 61 occur non-uniformly in a number of directions (cranio-caudal, medio-lateral, and  
189 62 ventro-dorsal) [9,10], uniplanar assessment of its size may be unreliable. It has been  
190 63 suggested that measurement of left atrial volume (LAV) on 2D echocardiography  
191 64 reduces these errors [11]. The American Society of Echocardiography recommends  
192 65 calculating LAV either by the disc summation algorithm (method of disk {MOD}), which  
193 66 is similar to the method for measuring left ventricular volume, or by an ellipsoid  
194 67 geometric model using the LA areas and lengths (area-length method {ALM}). Both  
195 68 techniques require two non-foreshortened left apical orthogonal views (two-chamber  
196 69 and four-chamber views) and are dependent on mathematical assumptions based on  
197 70 the LA having a fixed shaped. Consequently, they systematically underestimate LAV  
198 71 in people [12–15]. This has been overcome by the advent of new 3D imaging  
199 72 modalities such as real-time 3D echocardiography (RT-3DE) [16–20],  
200 73 electrocardiographic (ECG)-gated multi-detector computed tomography angiography  
201 74 (MDCTA) [13,21–25] and cardiac magnetic resonance imaging [12,25–27]. Left atrial  
202 75 volume obtained by 2D echocardiography offers limited accuracy. This is due to its  
203 76 reliance on geometric assumptions and the dependency on the view. To avoid LA  
204 77 foreshortening, two-chamber and four-chamber views should be truly orthogonal and  
205 78 optimised to maximise LA length and base in each view. Unlike 2D echocardiography,  
206  
207  
208  
209  
210  
211  
212  
213  
214  
215  
216  
217  
218  
219  
220  
221  
222  
223  
224  
225  
226  
227  
228  
229  
230  
231  
232  
233  
234  
235  
236

237  
238  
239  
240  
241  
242  
243  
244  
245  
246  
247  
248  
249  
250  
251  
252  
253  
254  
255  
256  
257  
258  
259  
260  
261  
262  
263  
264  
265  
266  
267  
268  
269  
270  
271  
272  
273  
274  
275  
276  
277  
278  
279  
280  
281  
282  
283  
284  
285  
286  
287  
288  
289  
290  
291  
292  
293  
294  
295

79 RT-3DE includes the entire LA within the 3D volume dataset and therefore is not  
80 subject to foreshortening, eliminates the limitations of geometric assumptions and thus  
81 reduces errors in volumetric measurement [10].

82 Furthermore, RT-3DE has good spatial and temporal resolution and, in people, has a  
83 greater correlation than its 2D counterpart with both ECG-gated cardiac magnetic  
84 resonance imaging and MDCTA, the current gold standards in volumetric  
85 measurement [12,24,25,27]. The introduction of new RT-3D transducers has resulted  
86 in sufficiently high frame rate image acquisition for veterinary clinical applications.  
87 Equally, post-processing analysis software using semi-automated border detection  
88 algorithms minimizes the initial learning curve and facilitates analysis [28,29].  
89 However, to date, RT-3DE assessment of LAV has only been validated in veterinary  
90 cardiology in one study including six healthy dogs [30].

91 We hypothesised that RT-3DE is more accurate than 2D echocardiography at  
92 calculating canine LAV. To investigate this hypothesis, we compared maximum LAV  
93 ( $LAV_{max}$ ) and minimum LAV ( $LAV_{min}$ ), measured by biplane ALM, biplane MOD and  
94 RT-3DE, with 64-slice ECG-gated MDCTA in dogs. Correlations between data sets  
95 were calculated and intra- and inter-observer variability in these methods were also  
96 determined.



296  
297  
298  
299  
300  
301  
302  
303  
304  
305  
306  
307  
308  
309  
310  
311  
312  
313  
314  
315  
316  
317  
318  
319  
320  
321  
322  
323  
324  
325  
326  
327  
328  
329  
330  
331  
332  
333  
334  
335  
336  
337  
338  
339  
340  
341  
342  
343  
344  
345  
346  
347  
348  
349  
350  
351  
352  
353  
354

97 **Animals, materials and methods**

98 **Enrolment**

99 This was a prospective study approved by our local ethics committee (Approval 45.17)  
100 and conducted at the Royal (Dick) School of Veterinary Studies between June 2017 –  
101 December 2017. Client-owned dogs were considered for enrolment if they had no  
102 history of cardiovascular disease and had been referred and scheduled for thoracic  
103 MDCTA under general anaesthesia. Informed client consent was obtained for every  
104 dog. Dogs were excluded if a murmur, arrhythmia or gallop rhythm was auscultated on  
105 physical examination. Dogs underwent oscillometric systolic blood pressure  
106 measurement<sup>a</sup>, blood sampling for routine haematology and serum biochemistry, and  
107 were anaesthetised using a standard protocol determined by a board-certified  
108 anaesthetist based on individual patient requirements. Premedicants included  
109 acepromazine<sup>b</sup>, partial<sup>c</sup> or full<sup>d</sup> opioid agonists and dexmedetomidine<sup>e</sup>. Anaesthesia  
110 was induced by intravenous propofol<sup>f</sup>, and maintained following endotracheal  
111 intubation by isoflurane<sup>g</sup> in oxygen. Electrocardiographic-gated MDCTA was  
112 performed, followed immediately by transthoracic echocardiography. Dogs were  
113 further excluded if a thoracic mass was seen to compress or displace the heart on  
114 ECG-gated MDCTA, or if congenital or acquired cardiac disease was detected on  
115 echocardiography. Mild valvular insufficiencies, in the absence of chamber  
116 enlargement, were permitted.

355  
356  
357  
358  
359  
360  
361  
362  
363  
364  
365  
366  
367  
368  
369  
370  
371  
372  
373  
374  
375  
376  
377  
378  
379  
380  
381  
382  
383  
384  
385  
386  
387  
388  
389  
390  
391  
392  
393  
394  
395  
396  
397  
398  
399  
400  
401  
402  
403  
404  
405  
406  
407  
408  
409  
410  
411  
412  
413

117 **Echocardiography**

118 Echocardiography<sup>h</sup> was performed under general anaesthesia by a single resident in  
119 cardiopulmonary medicine (JB), under the supervision of a board-certified cardiologist.  
120 Images were obtained with 4V-D (1.5 – 4.0 MHz)<sup>i</sup> and M5S-D (1.5 – 4.6 MHz)<sup>j</sup> matrix  
121 phased-array transducers during continuous ECG recording. Dogs were positioned  
122 alternatively in right and left lateral recumbency for transthoracic 2D, M-mode, pulsed-  
123 wave and continuous wave Doppler studies, and RT-3DE in accordance with the  
124 recommendations of the Echocardiography Committee of the Specialty of Cardiology  
125 of the American College of Veterinary Internal Medicine [31] and the American Society  
126 of Echocardiography [10,32]. Images were digitally stored and analysed offline with a  
127 commercially available software<sup>k</sup>.

128 **Electrocardiographic-gated multidetector computed tomography angiography**  
129 **image acquisition**

130 All MDCTA examinations were performed using a helical acquisition on a 64-slice  
131 MDCTA scanner<sup>l</sup>. A transverse plane examination of the thorax was performed using  
132 2 mm slice thickness and 1mm reconstruction interval, medium frequency  
133 reconstruction kernel, 80 kVp, 200 mA, 0.35 seconds tube rotation time and a  
134 collimator pitch of 0.51. Scan tube current was modulated by an automatic exposure  
135 control system<sup>m</sup>. A pre-monitoring transverse scan was set at the level of the aortic  
136 arch, and the automated bolus-tracking was set at 100 Hounsfield units with a cycle  
137 time of 3 seconds. A retrospectively ECG-gated cardiac MDCTA was performed using  
138 700 mg I/kg of iodinated contrast medium<sup>n</sup> followed by saline flush administered from  
139 a dual barrel injector<sup>o</sup> at 5 mL/s and 325 psi. Scan parameters used for the  
140 retrospectively gated scan were set to 1.25 mm slice thickness, 0.625 mm spacing

414  
415  
416 141 between slices, medium frequency reconstruction algorithm, field of view of 12 cm  
417  
418 142 centred over the heart, 80 kVp, 400 mA, 0.35 seconds tube rotation time and collimator  
419  
420  
421 143 pitch of 0.24.

## 422 423 144 **Measurement of left atrial size**

### 424 425 426 145 **Bi-dimensional echocardiography**

427  
428  
429 146 Angles of simultaneous multiplane 2D were adjusted to obtain left apical four- and two-  
430  
431 147 chamber views that maximised LA size to avoid foreshortening. Images were optimised  
432  
433 148 for endocardial visualisation and temporal and spatial resolution using the focus, depth,  
434  
435 149 sector size, frame rate, gain, compression, and time-gain compensation controls. All  
436  
437 150 measurements were performed at end-diastole (the frame just after mitral valve  
438  
439 151 closure) and end-systole (just before mitral valve opening) to obtain  $LA_{min}$  and  $LA_{max}$   
440  
441 152 respectively, according to American Society of Echocardiography guidelines [10]. Care  
442  
443 153 was taken to encompass the entire LA cavity in the data sets. The endocardial borders  
444  
445 154 were traced manually while excluding the left auricular appendage and the ostia of  
446  
447 155 pulmonary veins, if visible (Fig. 1). The mitral annulus was considered as the left  
448  
449 156 atrioventricular border. Three measurements were obtained and averaged for every  
450  
451 157 dog.

452  
453  
454  
455 158 Left atrial volume was calculated with the following formulae:

456  
457  
458 159 1) Area-length method calculation:  $LAV = \frac{8}{3\pi} \frac{(A_{4c} \times A_{2c})}{L_{min}}$

459  
460  
461 160 where  $A_{4c}$  is the area in the apical four-chamber view,  $A_{2c}$  is the area in the apical two-  
462  
463 161 chamber view, and  $L_{min}$  is the shorter length of the LA measured from the centre of the  
464  
465 162 mitral annular plane to the superior border of the chamber.

466  
467  
468 163 2) Method of disk calculation:  $LAV = \frac{\pi}{4} \sum_{i=1}^n (Di^{4c}) (Di^{2c}) \frac{L}{n} hi$

473  
474  
475 164 where  $h_i$  is the height of the stacked discs  $I_i$ , and  $D_{i4c}$  and  $D_{i2c}$  are two orthogonal minor  
476  
477 165 and major axes derived from four-chamber and two-chamber views respectively.  
478  
479

### 480 166 **Real-time three-dimensional echocardiography**

481  
482  
483 167 Three-dimensional cine loops were acquired over eight consecutive cardiac cycles  
484  
485 168 from the left parasternal view to obtain a single beat full-volume dataset with an  
486  
487 169 average frame rate of  $36.6 \pm 10.3$  frames per second (range 22.4 – 63 frames per  
488  
489 170 second). Loops were digitally stored and analysed offline with commercially available  
490  
491 171 software<sup>k,p</sup>. An effort was made to optimise image quality, increasing the frame rate by  
492  
493 172 narrowing the sector width and decreasing the depth. Maximum left atrial volume and  
494  
495 173  $LAV_{min}$  were derived from semi-automated tracing of the left atrial endocardium at end  
496  
497 174 ventricular systole and diastole respectively. The software<sup>k,p</sup> created an endocardial  
498  
499 175 cast of the left atrium, according to reference points on the hinge-point of the septal  
500  
501 176 leaflet, the hinge-points of the lateral leaflet, and the dorsal border of the left atrium  
502  
503 177 (Fig. 2, Supplemental video I, video available in Supplemental Material online). In all  
504  
505 178 cases, the cast was manually adjusted so that the plane of the mitral valve defined one  
506  
507 179 border, and the visual defect at the entry of the pulmonary veins was bridged. Care  
508  
509 180 was taken to approximate the entire LA endocardial border frame by frame through the  
510  
511 181 cardiac cycle. The pulmonary veins and left auricular appendage were not included.  
512  
513 182 Three measurements were obtained and averaged for each dog from three  
514  
515 183 representative cardiac cycles.  
516  
517  
518  
519

### 520 184 **Electrocardiographic-gated multidetector computed tomography angiography**

521  
522  
523 185 All assessments and measurements were performed by a diagnostic imaging resident  
524  
525 186 (FT) under board-certified veterinary radiologist (TS) supervision, using dedicated  
526  
527 187 DICOM viewer software<sup>q</sup>. A window width of 1700 Hounsfield units and a window level  
528  
529  
530  
531

532  
533  
534 188 of 200 Hounsfield units were used. The frames which depicted the  $LAV_{min}$  (just after  
535  
536 189 mitral valve closure) and  $LAV_{max}$  (just before mitral valve opening) were subjectively  
537  
538 190 determined on dynamic series using a 4D CINE mode review<sup>a</sup>. This mode allows  
539  
540 191 dynamic evaluation of a 3D image over time. Atrial volume analysis was performed by  
541  
542 192 drawing regions of interest, delineating the LA border. Initially, two slices were drawn  
543  
544 193 manually at each extremity of the LA, and the operator then drew slices between them  
545  
546 194 at random locations. Subsequently, the software generated several interconnecting  
547  
548 195 regions of interest (semi-automatic segmentation) that were adjusted manually to  
549  
550 196 ensure accuracy. Finally, the software calculated LAV by summing the volumes of all  
551  
552 197 the selected regions. The pulmonary veins and left auricular appendage were not  
553  
554 198 included. The anatomical limits of these structures were subjectively chosen by the  
555  
556 199 operator based on the contour of the LA as part of the semi-automatic segmentation  
557  
558 200 method (Fig. 3).  
559  
560  
561

### 562 201 **Variability analysis**

563  
564  
565 202 To calculate intra-observer within day and between day variabilities, six  
566  
567 203 echocardiograms and six MDCTA studies were randomly selected. Maximum left atrial  
568  
569 204 volume and  $LAV_{min}$  were measured by every method (ALM, MOD, 3D volume derived  
570  
571 205 from RT-3DE and ECG-gated MDCTA). The same cardiac cycle from the same cine  
572  
573 206 loops of every echocardiogram and every ECG-gated MDCTA were subjected to  
574  
575 207 repeated analyses by the same investigator (JB and FT respectively) at two different  
576  
577 208 time points on a given day (morning and afternoon) and on two different days.  
578  
579

580 209 The same images were used to evaluate inter-observer variability. Two independent  
581  
582 210 observers (YMP for echocardiography and JB for MDCTA) performed independent,  
583  
584 211 blinded and repeated analyses.  
585  
586  
587  
588  
589  
590

591  
592  
593  
594  
595  
596  
597  
598  
599  
600  
601  
602  
603  
604  
605  
606  
607  
608  
609  
610  
611  
612  
613  
614  
615  
616  
617  
618  
619  
620  
621  
622  
623  
624  
625  
626  
627  
628  
629  
630  
631  
632  
633  
634  
635  
636  
637  
638  
639  
640  
641  
642  
643  
644  
645  
646  
647  
648  
649

212 **Statistical analysis**

213 A sample size of 20 observations per group was estimated to give > 80% power to  
214 detect a correlation of at least 0.60 (with a critical p-value of 0.05) [33].  
215 Statistical analyses were performed using commercially available software<sup>r,s,t</sup>. Data  
216 were assessed for normality graphically and by use of the Shapiro-Wilk normality test.  
217 Continuous variables were reported as mean ± standard deviation. Correlations (r)  
218 between echocardiographic techniques and MDCTA were determined by Pearson's  
219 correlation test, and defined as excellent ( $r \geq 0.90$ ), very good ( $0.90 > r \geq 0.70$ ), good  
220 ( $0.70 > r \geq 0.50$ ) or poor ( $r < 0.50$ ) [34]. For sets of pairs of values, limits of agreement  
221 (LoA) and bias were assessed by Bland-Altman plots<sup>r</sup>, to visualise the comparisons  
222 graphically. Analysis of agreement was performed using intraclass correlation  
223 coefficient (ICC), assessing consistency of single measurement with a two-way model  
224 (as all methods were used on all cases) and corresponding 95% confidence intervals  
225 (CI), where 0 – 0.20 indicates poor agreement, 0.21 – 0.40 indicates fair agreement,  
226 0.41 – 0.60 indicates moderate agreement, 0.61 – 0.80 indicates substantial  
227 agreement, and > 0.80 indicates almost perfect agreement. These arbitrary cut-offs  
228 were similar to those used by Landis and Koch [35]. A p-value of less than 0.05 was  
229 considered to be statistically significant. Coefficients of variation were defined as the  
230 standard deviation of the differences divided by the mean of the variable under  
231 consideration, and were expressed as a percentage. Values <15% were considered  
232 adequate for clinical use [36].

650  
651  
652 **Results**  
653

654  
655 234 The study population consisted of 20 dogs of various breeds including cross breed (n  
656  
657 235 = 4), Labrador retriever (n = 3), golden retriever (n = 3), cocker spaniel (n = 2), and one  
658  
659 236 of each of the following breeds: flat coat retriever, schnauzer, rough collie, samoyed,  
660  
661 237 northern inuit, English springer spaniel, boxer and a border collie. There were four  
662  
663 238 intact females, six neutered females, six neutered males and four intact males. The  
664  
665 239 average age was  $7.45 \pm 4.14$  years (range 0.6 – 14.3 years). The average weight was  
666  
667 240  $26.3 \pm 9.3$  kg (range 9.1 – 44.5 kg) (supplemental Table A, data available in  
668  
669 241 Supplemental Material online). Table 1 displays selected descriptive statistics for  
670  
671 242  $LAV_{max}$  and  $LAV_{min}$  according to the method used to calculate LAV. Coefficients of  
672  
673 243 variation for within day, between day and inter-observer variability of the four methods  
674  
675 244 are listed in Table 2.

676  
677  
678  
679 245 **Real-time three-dimensional echocardiography and electrocardiographic-gated**  
680  
681 246 **multidetector computed tomography angiography**  
682

683  
684 247 Left atrial volume by RT-3DE was highly correlated with MDCTA for  $LAV_{max}$  ( $r = 0.94$ ,  
685  
686 248  $p < 0.0001$ ) and  $LAV_{min}$  ( $r = 0.82$ ,  $p < 0.0001$ ) (Fig. 4A and 4B respectively). However, on  
687  
688 249 Bland-Altman analysis, RT-3DE slightly underestimated  $LAV_{max}$  by 6% compared to  
689  
690 250 MDCTA (bias = -0.96 mL, 95% LoA: -5.6 – 3.7; Fig. 5A). Similarly, RT-3DE  
691  
692 251 underestimated  $LAV_{min}$  by 6.7% (bias = -0.67 mL, 95% LoA: -5.40 – 4.06; Fig. 5B).  
693  
694 252 Intraclass correlation (Table 3) confirmed these findings. There was almost perfect  
695  
696 253 agreement between ECG-gated MDCTA and RT-3DE for  $LAV_{max}$  (ICC = 0.93, CI: 0.83  
697  
698 254 – 0.97) and  $LAV_{min}$  (ICC = 0.82, CI: 0.60 – 0.93).  
699  
700

701  
702 255 **Two-dimensional echocardiography and electrocardiographic-gated**  
703  
704 256 **multidetector computed tomography angiography**  
705

709  
710  
711 257 Two-dimensional echocardiographic assessment of LAV also correlated well with  
712  
713 258 MDCTA but not as highly as RT-3DE ( $LAV_{max}$   $r = 0.81$  {MOD} and  $0.79$  {ALM}, both  
714  
715 259  $p < 0.0001$ , Fig. 4C and 4E; and  $LAV_{min}$   $r = 0.70$  {MOD} and  $0.72$  {ALM},  $p < 0.0006$  and  
716  
717  $p < 0.0004$  respectively, Fig. 4D and 4F). However, Bland Altman analysis showed that  
718  
719 261 MOD and ALM over-estimated  $LAV_{max}$  by 19.9% (bias = 3.18 mL, 95% LoA: -5.7 –  
720  
721 262 12.1) and 25.3% (bias = 4.05 mL, 95% LoA: -5.6 – 13.7) respectively (Fig. 5C and 5E).  
722  
723 263 Minimum left atrial volume, was also overestimated, by 19.4% for MOD (bias = 1.96  
724  
725 264 mL, 95% LoA: -4.6 – 8.5) and 27.7% for ALM (bias = 2.80 mL, 95% LoA: -3.9 – 9.5)  
726  
727 265 compared with MDCTA (Fig. 5D and 5F). The levels of agreement were less than that  
728  
729 266 obtained by 3D imaging. Values obtained by 2D echocardiography also demonstrated  
730  
731 267 substantial agreement with ECG-gated MDCTA for both  $LAV_{max}$  (ALM; ICC = 0.78, CI:  
732  
733 268 0.52 – 0.91; MOD; ICC = 0.71, CI: 0.40 – 0.87) and  $LAV_{min}$  (ALM; ICC = 0.80, CI: 0.56  
734  
735 269 – 0.92; MOD; ICC = 0.70, CI: 0.38 – 0.87).  
736  
737  
738

## 739 270 **Discussion**

740  
741  
742 271 Real-time three-dimensional echocardiography is a new technique whose innovative  
743  
744 272 use in people to quantify LAV has greatly expanded over the last decade. Multiple  
745  
746 273 human studies have consistently shown that RT-3DE is a useful diagnostic tool that  
747  
748 274 tends to underestimate LAV to a lesser extent than biplane ALM or MOD [12,13,24,27].  
749  
750 275 This is the first veterinary study to measure the degrees of accuracy and bias of a  
751  
752 276 commercially available 3D echocardiography system, using semi-automated border  
753  
754 277 detection to measure LAV in a population of canine patients.  
755  
756 278 We have demonstrated that RT-3DE in dogs is more accurate at measuring LAV than  
757  
758 279 2D echocardiography when compared with the gold standard of 64-slice ECG-gated  
759  
760 280 MDCTA. Real-time three-dimensional echocardiography-derived values were in  
761  
762 281 almost perfect agreement with those obtained by MDCTA, whereas 2D methods  
763  
764  
765  
766  
767



768  
769  
770 282 overestimated LAV with wider LoA. In agreement with the recent work of Tidholm et al.  
771  
772 283 (2019), we conclude that 2D volume-based methods and RT-3DE cannot be used  
773  
774 284 interchangeably to quantify LAV in dogs [37]. Although 2D measurements remain  
775  
776 285 easier and quicker to perform, RT-3DE is feasible, more accurate, and highly  
777  
778 286 reproducible, so that establishing canine reference ranges is a realistic goal.  
780  
781 287 We used an ECG-gated MDCTA volumetric gold standard because it is used to  
782  
783 288 measure LAV in people with a high degree of accuracy, even when they have atrial  
784  
785 289 fibrillation [24,25,38,39]. Furthermore, in dogs, ECG-gated MDCTA is already  
786  
787 290 recognised as a volumetric gold standard for assessment of left and right ventricular  
788  
789 291 volumes [40,41].  
790  
791 292 Accuracy of echocardiographic methods was determined in two stages. First, both RT-  
792  
793 293 3DE and 2D echocardiography were shown to correlate highly with the volumetric gold  
794  
795 294 standard. Second, Bland-Altman plots confirmed that RT-3DE outperformed 2DE with  
796  
797 295 a minimal bias and the narrowest 95% LoA obtained for both  $LAV_{max}$  and  $LAV_{min}$ . The  
798  
799 296 slight underestimation of RT-3DE that we recorded is consistent with reported biases  
800  
801 297 in human medicine ranging from 0 to -2.5 mL [12,24].  
802  
803 298 Studies in people have consistently shown that 2D echocardiography, as well as RT-  
804  
805 299 3DE, underestimates LAV compared to gold standard methods [12,13,15,20,24–27].  
806  
807 300 Surprisingly, in our study, we found that 2D planimetric methods overestimated LAV.  
808  
809 301 The reason for this is unclear. It could be that differences in thoracic conformation and  
810  
811 302 anatomical cardiac chamber anatomy mean that geometric assumptions that are valid  
812  
813 303 in people do not apply to the canine LA [42]. Importantly, this discrepancy illustrates  
814  
815 304 the pitfalls of extrapolating data across species when applying novel imaging  
816  
817 305 modalities to veterinary medicine.  
818  
819  
820  
821  
822  
823  
824  
825  
826

827  
828  
829 306 Two previous veterinary studies broadly agree with our data. They also demonstrated  
830  
831 307 overestimation of LAV by both 2D planimetric methods, compared to RT-3DE [18] or  
832  
833 308 cardiac magnetic resonance imaging [30], although cardiac magnetic resonance  
834  
835 309 imaging does not appear to correlate with monoplane MOD, RT-3DE or even MDCTA.  
836  
837  
838 310 Furthermore, and similar to people [22,43,44], our MOD-derived values were closer to  
839  
840 311 MDCTA values than ALM-derived ones, since biplane MOD makes fewer geometric  
841  
842 312 assumptions than ALM [10]. This would suggest that in healthy dogs, although inferior  
843  
844 313 to RT-3DE, biplane MOD remains the 2D planimetric method of choice for measuring  
845  
846 314 LAV [10,37,43]. By contrast, in a recent Swedish study that included a large population  
847  
848 315 of dogs with myxomatous mitral valve disease, biplane MOD underestimated LAV  
849  
850 316 compared to RT-3DE [37]. Our data suggest that 2D geometric assumptions might be  
851  
852 317 less accurate in dogs with bigger atria since there was a trend towards an increase in  
853  
854 318 the scatter of the difference between MDCTA and planimetric measurements of LAV  
855  
856 319 as atrial size increased.  
857  
858  
859 320 Reduced accuracy at bigger LAV may relate to the views from which images were  
860  
861 321 derived. Both RT-3DE and 2D images were obtained from left apical views. Apical  
862  
863 322 imaging places LA in a far field of the ultrasound beam, leading to loss of lateral  
864  
865 323 resolution, poor visualisation, and inaccurate tracing of the LA endocardial border  
866  
867 324 [22,45]. Despite significant effort by the sonographer to obtain good quality non-  
868  
869 325 foreshortened four- and two-chamber views by optimising the width and the depth,  
870  
871 326 manual tracing errors may have contributed to LAV overestimation by including some  
872  
873 327 of the LAA or pulmonary veins [46]. Indeed, unlike in people, canine pulmonary veins  
874  
875 328 anastomose into a cone-shaped trunk prior to entering the LA. This leads to an  
876  
877 329 imprecise delineation between left atrial tissue and the beginning of pulmonary veins  
878  
879 330 [42]. By contrast, in RT-3DE, we used a semi-automated software package designed  
880  
881  
882  
883  
884  
885

886  
887  
888 331 to provide an ellipsoidal 3D cast of the left ventricle after placing three references points  
889  
890 332 on the endocardial border. Although this required manual adjustment, the degree of  
891  
892 333 manual involvement was significantly less than with 2D techniques. It is possible that  
893  
894 334 the software package is superior to manual selection of border delineation, resulting in  
895  
896  
897 335 greater inaccuracy where there is greater manual input i.e. 2D methods. Indeed,  
898  
899 336 manual tracing of the endocardium is operator-dependant and tends to be associated  
900  
901 337 with higher interobserver variability than RT-3DE [20]. Despite the reproducibility  
902  
903 338 among the echocardiographic methods in our study being <15%, and hence clinically  
904  
905 339 acceptable compared to previously reported human [12,20,24] and veterinary  
906  
907 340 [18,43,47] studies, the effect size would be greater with bigger left atria, which have  
908  
909 341 longer perimeters. We conclude that despite the advantages of RT-3DE over 2D  
910  
911 342 imaging, RT-3DE requires separate validation for measuring LAV in disease states,  
912  
913 343 using a large population of dogs.  
914  
915 344 These findings are clinically significant, since thoracic conformation can vary greatly in  
916  
917 345 dogs of different morphotypes potentially leading to anatomical variation, including LAV  
918  
919 346 [48,49]. Indeed, Hollmer et al. (2013) have documented significant breed-related  
920  
921 347 differences in LAV using the biplane ALM in dogs with normal cardiovascular status  
922  
923 348 [47]. By contrast, we demonstrated that RT-3DE maintained its bias over a range of  
924  
925 349 LAV within brachycephalic, dolicocephalic and mesaticephalic breeds with slight  
926  
927 350 underestimation. We speculate that RT-3DE would also demonstrate the same bias  
928  
929 351 and degree of accuracy within breeds over a range of pathological LA remodelling.  
930  
931 352 Additional research validating the use of RT-3DE measurements in dogs with enlarged  
932  
933 353 left atria is warranted to confirm this hypothesis.  
934  
935  
936  
937 354

945  
946  
947 355 Our study has several noteworthy limitations that should be considered. It was not  
948  
949 356 designed to correct for potential confounders such as heart rate, changes in LA loading  
950  
951 357 conditions, sex, image quality and eventually variability throughout the breathing cycle,  
952  
953 358 and no attempts were made to correlate these parameters with LAV. Sporadically, we  
954  
955 359 found that sinus arrhythmia or heart rates greater than 80 beats per minute caused  
956  
957 360 stair-step and motion artefacts on MDCTA. This was due to the limited temporal  
958  
959 361 resolution of 64-slice ECG-gated MDCTA and the absence of breath holding during  
960  
961 362 data acquisition. The consequence was poorer definition of the LA endocardial border,  
962  
963 363 although we believe that this was not sufficient to lead to erroneous measurements  
964  
965 364 because each patient served as his own control with short time-frame between  
966  
967 365 modalities and therefore data acquisitions.

970  
971 366 The confounding effects on respirophasic changes are likely to have been similar  
972  
973 367 between the different methods used to measure LAV [50]. Lung expansion during end-  
974  
975 368 inspiration decreases LAV, and conversely, LAV increases during end-expiration  
976  
977 369 [50,51]. In our study, anaesthetised dogs were assisted by mechanical ventilation  
978  
979 370 during both MDCTA and echocardiography. Images acquisition were not synchronised  
980  
981 371 with the breathing cycle, which could theoretically influenced the loading condition of  
982  
983 372 the LA. Synchronisation with the breathing cycle would have imply using breath-  
984  
985 373 holding which was not undertaken not only for ethical reasons but also to mirror clinical  
986  
987 374 situations. Besides, breath-holding could have influenced the loading of the LA by up  
988  
989 375 to 20% compared to normal breathing [52].

991  
992 376 Real-time three-dimensional echocardiography is also subject to limited temporal and  
993  
994 377 spatial resolution during real-time acquisition. In previous veterinary studies, the  
995  
996 378 optimal balance between spatial and temporal resolution was obtained by acquiring  
997  
998 379 volume datasets with multi-beat modalities involving acquisition of four to seven  
999

1004  
1005  
1006  
1007  
1008  
1009  
1010  
1011  
1012  
1013  
1014  
1015  
1016  
1017  
1018  
1019  
1020  
1021  
1022  
1023  
1024  
1025  
1026  
1027  
1028  
1029  
1030  
1031  
1032  
1033  
1034  
1035  
1036  
1037  
1038  
1039  
1040  
1041  
1042  
1043  
1044  
1045  
1046  
1047  
1048  
1049  
1050  
1051  
1052  
1053  
1054  
1055  
1056  
1057  
1058  
1059  
1060  
1061  
1062

380 cardiac cycles [16–18,53]. However, to avoid stitching artefact, this mode requires a  
381 regular heart rate (ideally between 60 and 90 beats per minute based on the author  
382 experience), breath-holding and stable probe handling from the operator. This is not  
383 easily achieved in a clinical veterinary setting. Our aim was to demonstrate the clinical  
384 feasibility of RT-3DE, and because inhalation anaesthetics can increase heart rate by  
385 decreasing cardiac vagal activity [54], single-beat acquisition was preferred at the  
386 expense of image quality. Overall image quality was deemed adequate for LAV  
387 estimation and our conclusions should be equally applicable to emerging 3D  
388 technologies with improved image quality.

389 It is also worth emphasising that frame selection varied due to image quality and frame  
390 rate. Consequently, measurements were not performed at exactly the same time point,  
391 potentially leading to underestimation of LA. However, we attempted to overcome this  
392 limitation by relying on the average of three different measurements for each variable  
393 for both MDCTA and RT-3DE.

394 The aim of this study was not to generate allometric relationships in order to establish  
395 reference values for RT-3DE and planimetric methods. Additional studies involving the  
396 use of RT-3DE in a larger population of dogs are required to establish reference values  
397 in healthy and conscious patients, and to optimise the clinical utility of RT-3DE to  
398 estimate LAV.

399 **Conclusions**

400 This is the first prospective study in veterinary medicine to study the accuracy and the  
401 bias of RT-3DE with a volumetric gold standard to estimate LAV. Three-dimensional-  
402 derived LAV measurements were found to be feasible, reproducible and more accurate  
403 than 2D echocardiography-based volumetric methods. Our results might facilitate  
404 future clinical research in order to determine a general consensus for the best method

1063  
1064  
1065  
1066  
1067  
1068  
1069  
1070  
1071  
1072  
1073  
1074  
1075  
1076  
1077  
1078  
1079  
1080  
1081  
1082  
1083  
1084  
1085  
1086  
1087  
1088  
1089  
1090  
1091  
1092  
1093  
1094  
1095  
1096  
1097  
1098  
1099  
1100  
1101  
1102  
1103  
1104  
1105  
1106  
1107  
1108  
1109  
1110  
1111  
1112  
1113  
1114  
1115  
1116  
1117  
1118  
1119  
1120  
1121

405 to assess LAV. Although RT-3DE is not currently widely available in veterinary  
406 medicine, this modality remains appealing and holds promise for LAV assessment. It  
407 is anticipated that this imaging modality will emerge as a powerful diagnostic tool and  
408 will be integrated into clinical guidelines and routine practice as the imaging modality  
409 of choice for LA assessment with dedicated software and adapted algorithms  
410 alongside the improvement of spatial and temporal resolution in the next generation of  
411 3D probes.

**Conflicts of Interest Statement**

The authors do not have any conflicts of interest to disclose

1122  
1123  
1124  
1125  
1126  
1127  
1128  
1129  
1130  
1131  
1132  
1133  
1134  
1135  
1136  
1137  
1138  
1139  
1140  
1141  
1142  
1143  
1144  
1145  
1146  
1147  
1148  
1149  
1150  
1151  
1152  
1153  
1154  
1155  
1156  
1157  
1158  
1159  
1160  
1161  
1162  
1163  
1164  
1165  
1166  
1167  
1168  
1169  
1170  
1171  
1172  
1173  
1174  
1175  
1176  
1177  
1178  
1179  
1180

414 Footnotes

- 415 a. Cardell Model 9402, CAS Medical Systems, Brandford, Connecticut.
- 416 b. Acecare, Animalcare limited, United Kingdom
- 417 c. Alvegesic, Dechra Veterinary products, United Kingdom
- 418 d. Comfortan, Dechra Veterinary products, United Kingdom
- 419 e. Dexmedetomidine, Orion Pharma, Turku, Finland
- 420 f. Propoflo plus, Zoetis UK Ltd, United Kingdom
- 421 g. Isocare, Animalcare Ltd, United Kingdom
- 422 h. Vivid E9, General Electric Medical Systems, Waukesha, Wisconsin.
- 423 i. 4V-D Active Matrix 4D Volume Phased Array Transducer 1.5 – 4.0MHz
- 424 j. M5S-D Active Matrix single-crystal Phased Array Transducer 1.5 – 4.6MHz
- 425 k. EchoPAC PC versions 113, GE Healthcare, Horten, Norway
- 426 l. Somatom Sensation 64, Siemens Medical Solutions, Erlangen, Germany.
- 427 m. Care Dose 4D®, Siemens Healthcare, Forchheim, Germany
- 428 n. Niopam 350®, Bracco UK Ltd, United Kingdom
- 429 o. Empower CTA®, Bracco® injeneering S.A., Milan, Italy
- 430 p. 4D-AutoLVQ, GE Healthcare, Horten, Norway
- 431 q. OsiriX v5.8.5 64-bit, Geneva, Switzerland
- 432 r. GraphPad Prism version 7.00 for Windows, GraphPad Software, La Jolla,  
433 California, USA.
- 434 s. Minitab 17, Pennsylvania, USA
- 435 t. MedClac Stasticial Software, version 18.5, MedCalc Software bvba, Ostend,  
436 Belgium

1181  
1182  
1183  
1184  
1185  
1186  
1187  
1188  
1189  
1190  
1191  
1192  
1193  
1194  
1195  
1196  
1197  
1198  
1199  
1200  
1201  
1202  
1203  
1204  
1205  
1206  
1207  
1208  
1209  
1210  
1211  
1212  
1213  
1214  
1215  
1216  
1217  
1218  
1219  
1220  
1221  
1222  
1223  
1224  
1225  
1226  
1227  
1228  
1229  
1230  
1231  
1232  
1233  
1234  
1235  
1236  
1237  
1238  
1239

438 REFERENCES

439 [1] Borgarelli M, Santilli RA, Chiavegato D, D'Agnolo G, Zanatta R, Mannelli A,  
440 Tarducci A. Prognostic Indicators for Dogs with Dilated Cardiomyopathy. *J Vet*  
441 *Intern Med* 2006;20:104–10.

442 [2] Borgarelli M, Savarino P, Crosara S, Santilli RA, Chiavegato D, Poggi M,  
443 Bellino C, La Rosa G, Zanatta R, Haggstrom J, Tarducci A. Survival  
444 Characteristics and Prognostic Variables of Dogs with Mitral Regurgitation  
445 Attributable to Myxomatous Valve Disease. *J Vet Intern Med* 2008;22:120–8.

446 [3] Rossi A, Cicoira M, Zanolla L, Sandrini R, Golia G, Zardini P, Enriquez-Sarano  
447 M. Determinants and prognostic value of left atrial volume in patients with  
448 dilated cardiomyopathy. *J Am Coll Cardiol* 2002;40:1425–30.

449 [4] Sargent J, Muzzi R, Mukherjee R, Somarathne S, Schranz K, Stephenson H,  
450 Connoly D, Brodbelt D, Luis Fuentes V. Echocardiographic predictors of  
451 survival in dogs with myxomatous mitral valve disease. *J Vet Cardiol*  
452 *2015;17:1–12.*

453 [5] Wu VC-C, Takeuchi M, Kuwaki H, Iwataki M, Nagata Y, Otani K, Haruki N,  
454 Yoshitani H, Tamura N, Abe H, Negishi K, Lin FC, Otsuji Y. Prognostic value of  
455 LA volumes assessed by transthoracic 3D echocardiography. *J Am Coll*  
456 *Cardiol Img* 2013;6:1025–35.

457 [6] Rishniw M, Erb HN. Evaluation of four 2-dimensional echocardiographic  
458 methods of assessing left atrial size in dogs. *J Vet Intern Med* 2000;14:429–35.

459 [7] Hansson K, Haggstrom J, Kvart C, Lord P. Left atrial to aortic root indices using  
460 two-dimensional and M-mode echocardiography in cavalier King Charles  
461 spaniels with and without left atrial enlargement. *Vet Radiol Ultrasound*  
462 *2002;43:568–75.*



1240  
1241  
1242  
1243  
1244  
1245  
1246  
1247  
1248  
1249  
1250  
1251  
1252  
1253  
1254  
1255  
1256  
1257  
1258  
1259  
1260  
1261  
1262  
1263  
1264  
1265  
1266  
1267  
1268  
1269  
1270  
1271  
1272  
1273  
1274  
1275  
1276  
1277  
1278  
1279  
1280  
1281  
1282  
1283  
1284  
1285  
1286  
1287  
1288  
1289  
1290  
1291  
1292  
1293  
1294  
1295  
1296  
1297  
1298

463 [8] De Madron É. Normal Echocardiographic Values. In: De Madron É, Chetboul  
464 V, Bussadori C, editors. Clinical echocardiography of the dog and cat. St.  
465 Louis: Elsevier; 2015, p. 21–37.

466 [9] Wesselowski S, Borgarelli M, Bello NM, Abbott J. Discrepancies in  
467 identification of left atrial enlargement using left atrial volume versus left atrial-  
468 to-aortic root ratio in dogs. J Vet Intern Med 2014;28:1527–33.

469 [10] Lang RM, Badano LP, Mor-Avi V, Afilalo J, Armstrong A, Ernande L,  
470 Flachskampf FA, Foster E, Goldstein SA, Kuznetsova T, Lancellotti P, Muraru  
471 D, Picard MH, Rietzschel ER, Rudski L, Spencer KT, Tsang W, Voigt J-U.  
472 Recommendations for cardiac chamber quantification by echocardiography in  
473 adults: an update from the American Society of Echocardiography and the  
474 European Association of Cardiovascular Imaging. Eur Hear J Cardiovasc  
475 Imaging 2015;16:233–71.

476 [11] Vizzardi E, D’Aloia A, Rocco E, Lupi L, Rovetta R, Quinzani F, Bontempi L,  
477 Curnis A, Dei Cas L. How should we measure left atrium size and function? J  
478 Clin Ultrasound 2012;40:155–66.

479 [12] Mor-Avi V, Yodwut C, Jenkins C, Kühl H, Nesser H-J, Marwick TH, Franke A,  
480 Weinert L, Niel J, Steringer-Mascherbauer R, Free BH, Sugeng L, Lang R.  
481 Real-time 3D echocardiographic quantification of left atrial volume. J Am Coll  
482 Cardiol Img 2012;5:769–77.

483 [13] Koka AR, Gould SD, Owen AN, Halpern EJ. Left atrial volume: comparison of  
484 2D and 3D transthoracic echocardiography with ECG-gated CT angiography.  
485 Acad Radiol 2012;19:62–8.

486 [14] Maddukuri P V, Vieira MLC, DeCastro S, Maron MS, Kuvin JT, Patel AR, Patel  
487 AR, Pandian NG. What is the best approach for the assessment of left atrial

1299  
1300  
1301  
1302  
1303  
1304  
1305  
1306  
1307  
1308  
1309  
1310  
1311  
1312  
1313  
1314  
1315  
1316  
1317  
1318  
1319  
1320  
1321  
1322  
1323  
1324  
1325  
1326  
1327  
1328  
1329  
1330  
1331  
1332  
1333  
1334  
1335  
1336  
1337  
1338  
1339  
1340  
1341  
1342  
1343  
1344  
1345  
1346  
1347  
1348  
1349  
1350  
1351  
1352  
1353  
1354  
1355  
1356  
1357

488 size? Comparison of various unidimensional and two-dimensional parameters  
489 with three-dimensional echocardiographically determined left atrial volume. J  
490 Am Soc Echocardiogr 2006;19:1026–32.

[15] 491 Al-Mohaissen MA, Kazmi MH, Chan KL, Chow BJW. Validation of two-  
492 dimensional methods for left atrial volume measurement: A comparison of  
493 echocardiography with cardiac computed tomography. Echocardiography  
494 2013;30:1135–42.

[16] 495 Tidholm A, Bodegård-Westling A, Höglund K, Ljungvall I, Häggström J.  
496 Comparisons of 2- and 3-dimensional echocardiographic methods for  
497 estimation of left atrial size in dogs with and without myxomatous mitral valve  
498 disease. J Vet Intern Med 2011;25:1320–7.

[17] 499 Tidholm A, Höglund K, Häggström J, Bodegård-Westling A, Ljungvall I. Left  
500 atrial ejection fraction assessed by real-time 3-dimensional echocardiography  
501 in normal dogs and dogs with myxomatous mitral valve disease. J Vet Intern  
502 Med 2013;27:884–9.

[18] 503 LeBlanc N, Scollan K, Sisson D. Quantitative evaluation of left atrial volume  
504 and function by one-dimensional, two-dimensional, and three-dimensional  
505 echocardiography in a population of normal dogs. J Vet Cardiol 2016;18:336–  
506 49.

[19] 507 Jenkins C, Bricknell K, Marwick TH. Use of Real-time Three-dimensional  
508 echocardiography to measure left atrial volume: Comparison with other  
509 echocardiographic techniques. J Am Soc Echocardiogr 2005;18:991–7.

[20] 510 Badano LP, Miglioranza MH, Mihăilă S, Peluso D, Xhaxho J, Marra MP,  
511 Cucchini U, Soriani N, Iliceto S, Muraru D. Left atrial volumes and function by  
512 three-dimensional echocardiography. Circ Cardiovasc Imaging

1358  
1359  
1360  
1361  
1362  
1363  
1364  
1365  
1366  
1367  
1368  
1369  
1370  
1371  
1372  
1373  
1374  
1375  
1376  
1377  
1378  
1379  
1380  
1381  
1382  
1383  
1384  
1385  
1386  
1387  
1388  
1389  
1390  
1391  
1392  
1393  
1394  
1395  
1396  
1397  
1398  
1399  
1400  
1401  
1402  
1403  
1404  
1405  
1406  
1407  
1408  
1409  
1410  
1411  
1412  
1413  
1414  
1415  
1416

513 2016;9:e004229.

514 [21] Gweon HM, Kim SJ, Kim TH, Lee SM, Hong YJ, Rim S-J. Evaluation of left  
515 atrial volumes using multidetector computed tomography: Comparison with  
516 echocardiography. *Korean J Radiol* 2010;11:286.

517 [22] Takagi Y, Ehara S, Okuyama T, Shirai N, Yamashita H, Sugioka K, Kitamura  
518 H, Ujino K, Hozumi T, Yoshiyama M. Comparison of determinations of left atrial  
519 volume by the biplane area-length and Simpson's methods using 64-slice  
520 computed tomography. *J Cardiol* 2009;53:257–64.

521 [23] Mahabadi AA, Samy B, Seneviratne SK, Toepker MH, Bamberg F, Hoffmann  
522 U, Truong QA. Quantitative assessment of left atrial volume by  
523 electrocardiographic-gated contrast-enhanced multidetector computed  
524 tomography. *J Cardiovasc Comput Tomogr* 2009;3:80–7.

525 [24] Miyasaka Y, Tsujimoto S, Maeba H, Yuasa F, Takehana K, Dote K, Iwasaka T.  
526 Left atrial volume by real-time three-dimensional echocardiography: Validation  
527 by 64-slice multidetector computed tomography. *J Am Soc Echocardiogr*  
528 2011;24:680–6.

529 [25] Kühl JT, Lønborg J, Fuchs A, Andersen MJ, Vejlstrup N, Kelbæk H, Engstrøm  
530 T, Møller JE, Kofoed K. Assessment of left atrial volume and function: A  
531 comparative study between echocardiography, magnetic resonance imaging  
532 and multi slice computed tomography. *Int J Cardiovasc Imaging* 2012;28:1061–  
533 71.

534 [26] Rodevand O, Bjornerheim R, Ljosland M, Maehle J, Smith HJ, Ihlen H. Left  
535 atrial volumes assessed by three- and two-dimensional echocardiography  
536 compared to MRI estimates. *Int J Cardiovasc Imaging* 1999;15:397–410.

537 [27] Artang R, Migrino RQ, Harmann L, Bowers M, Woods TD. Left atrial volume

1417  
1418  
1419 538 measurement with automated border detection by 3-dimensional  
1420  
1421 539 echocardiography: Comparison with magnetic resonance imaging. *Cardiovasc*  
1422  
1423 *Ultrasound* 2009;7:16.  
1424 540  
1425  
1426 541 [28] Chin RB, Tighe C, Beaver T, Welch T, Costa S. Advances in 3D  
1427  
1428 542 echocardiography: Automated software improves the learning curve and  
1429  
1430 543 clinical implementation in a real world setting for quantitative assessment of left  
1431  
1432 544 ventricular ejection. *J Am Coll Cardiol* 2017;69:1642.  
1433  
1434 545 [29] Tsang W, Salgo IS, Medvedofsky D, Takeuchi M, Prater D, Weinert L, Yamat  
1435  
1436 546 M, Mor-Avi V, Patel A, Lang R. Transthoracic 3D echocardiographic left heart  
1437  
1438 547 chamber quantification using an automated adaptive analytics algorithm. *J Am*  
1439  
1440 548 *Coll Cardiol Img* 2016;9:769–82.  
1441  
1442  
1443 549 [30] Fries RC, Gordon SG, Saunders AB, Miller MW, Hariu CD, Schaeffer DJ.  
1444  
1445 550 Quantitative assessment of two- and three-dimensional transthoracic and two-  
1446  
1447 551 dimensional transesophageal echocardiography , computed tomography , and  
1448  
1449 552 magnetic resonance imaging in normal canine hearts. *J Vet Cardiol*  
1450  
1451 553 2019;21:79–92.  
1452  
1453 554 [31] Thomas WP, Gaber CE, Jacobs GJ, Kaplan PM, Lombard CW, Moise NS,  
1454  
1455 555 Moses BL. Recommendations for standards in transthoracic two-dimensional  
1456  
1457 556 echocardiography in the dog and cat. Echocardiography Committee of the  
1458  
1459 557 Specialty of Cardiology, American College of Veterinary Internal Medicine. *J*  
1460  
1461 558 *Vet Intern Med* 1993;7:247–52.  
1462  
1463  
1464 559 [32] Quiñones MA, Otto CM, Stoddard M, Waggoner A, Zoghbi WA.  
1465  
1466 560 Recommendations for quantification of Doppler echocardiography: A report  
1467  
1468 561 from the Doppler quantification task force of the nomenclature and standards  
1469  
1470 562 committee of the American Society of Echocardiography. *J Am Soc*

1476  
1477  
1478 563 Echocardiogr 2002;15:167–84.  
1479  
1480 564 [33] Browner WS, Newman TB, Hulley SB. Estimating sample size and power:  
1481  
1482 applications and examples. In: Hulley SB, Cummings SR, Browner WS, Grady  
1483 565  
1484 D, Newman TB, editors. Designing clinical research : an epidemiologic  
1485 566  
1486 approach. 4th ed, Philadelphia: Lippincott Williams & Wilkins; 2013, p. 79  
1487 567  
1488 appendix 6C.  
1489 568  
1490  
1491 569 [34] Hinkle DE, Wiersma W, Jurs SG. Rule of thumb for interpreting the size of a  
1492  
1493 correlation coefficient. In: Hinkle DE, Wiersma W, Jurs SG , editors. Applied  
1494 570  
1495 statistics for the behavioral sciences. 5th ed. Boston: Houghton Mifflin; 2003.  
1496 571  
1497  
1498 572 [35] Landis JR, Koch GG. The measurement of observer agreement for categorical  
1499  
1500 data. Biometrics 1977;33:159–74.  
1501  
1502 574 [36] Chetboul V. Intra- and Interoperator Variability. In: De Madron É, Chetboul V,  
1503  
1504 Bussadori C, editors. Clinical echocardiography of the dog and cat. St. Louis:  
1505 575  
1506 Elsevier; 2015, p. 39–43.  
1507  
1508 577 [37] Tidholm A, Bodegård-Westling A, Höglund K, Häggström J, Ljungvall I.  
1509  
1510 Comparison between real-time 3-dimensional and 2-dimensional biplane  
1511 578  
1512 echocardiographic assessment of left atrial volumes in dogs with myxomatous  
1513 579  
1514 mitral valve disease. J Vet Intern Med 2019;33(2):455–61.  
1515 580  
1516  
1517 581 [38] Agner BFR, Kühl JT, Linde JJ, Kofoed KF, Akeson P, Rasmussen BV, Jensen  
1518  
1519 GB, Dixen U. Assessment of left atrial volume and function in patients with  
1520 582  
1521 permanent atrial fibrillation: comparison of cardiac magnetic resonance  
1522 583  
1523 imaging, 320-slice multi-detector computed tomography, and transthoracic  
1524 584  
1525 echocardiography. Eur Heart J Cardiovasc Imaging 2014;15:532–40.  
1526 585  
1527 586 [39] Rohner A, Brinkert M, Kawel N, Buechel RR, Leibundgut G, Grize L, Kühne M,  
1528  
1529 Bremerich J, Kaufmann BA, Zellweger MJ, Buser P, Osswald S, Handke M.  
1530 587  
1531  
1532  
1533  
1534

1535  
1536  
1537 588 Functional assessment of the left atrium by real-time three-dimensional  
1538  
1539 589 echocardiography using a novel dedicated analysis tool: initial validation  
1540  
1541 590 studies in comparison with computed tomography. *Eur Heart J Cardiovasc*  
1542  
1543 591 *Imaging* 2011;12:497–505.  
1544  
1545  
1546 592 [40] Scollan KF, Stieger-Vanegas SM, Sisson DD. Assessment of left ventricular  
1547  
1548 593 volume and function in healthy dogs by use of one-, two-, and three-  
1549  
1550 594 dimensional echocardiography versus multidetector computed tomography. *Am*  
1551  
1552 595 *J Vet Res* 2016;77:1211–9.  
1553  
1554 596 [41] Sieslack AK, Dziallas P, Nolte I, Wefstaedt P, Hungerbühler SO. Quantification  
1555  
1556 597 of right ventricular volume in dogs: a comparative study between three-  
1557  
1558 598 dimensional echocardiography and computed tomography with the reference  
1559  
1560 599 method magnetic resonance imaging. *BMC Vet Res* 2014;10:242.  
1561  
1562  
1563 600 [42] Brewer FC, Moïse NS, Kornreich BG, Bezuidenhout AJ. Use of computed  
1564  
1565 601 tomography and silicon endocasts to identify pulmonary veins with  
1566  
1567 602 echocardiography. *J Vet Cardiol* 2012;14:293–300.  
1568  
1569 603 [43] Höllmer M, Willesen JL, Tolver A, Koch J. Comparison of four  
1570  
1571 604 echocardiographic methods to determine left atrial size in dogs. *J Vet Cardiol*  
1572  
1573 605 2016;18:137–45.  
1574  
1575 606 [44] Jiamsripong P, Honda T, Reuss C, Hurst R, Chaliki H, Grill D, Schnek SL, Tyler  
1576  
1577 607 R, Khandheria BK, Lester SJ. Three methods for evaluation of left atrial  
1578  
1579 608 volume. *Eur J Echocardiogr* 2007;9:351–5.  
1580  
1581  
1582 609 [45] Lester SJ, Ryan EW, Schiller NB, Foster E. Best method in clinical practice and  
1583  
1584 610 in research studies to determine left atrial size. *Am J Cardiol* 1999;84:829–32.  
1585  
1586 611 [46] Russo C, Hahn RT, Jin Z, Homma S, Sacco RL, Di Tullio MR. Comparison of  
1587  
1588 612 echocardiographic single-plane versus biplane method in the assessment of

1594  
1595  
1596  
1597  
1598  
1599  
1600  
1601  
1602  
1603  
1604  
1605  
1606  
1607  
1608  
1609  
1610  
1611  
1612  
1613  
1614  
1615  
1616  
1617  
1618  
1619  
1620  
1621  
1622  
1623  
1624  
1625  
1626  
1627  
1628  
1629  
1630  
1631  
1632  
1633  
1634  
1635  
1636  
1637  
1638  
1639  
1640  
1641  
1642  
1643  
1644  
1645  
1646  
1647  
1648  
1649  
1650  
1651  
1652

613 left atrial volume and validation by real time three-dimensional  
614 echocardiography. *J Am Soc Echocardiogr* 2010;23:954–60.

615 [47] Höllmer M, Willesen JL, Tolver A, Koch J. Left atrial volume and phasic  
616 function in clinically healthy dogs of 12 different breeds. *Vet J* 2013;197:639–  
617 45.

618 [48] Evans E. H, De Lahunta A. The Skeleton. In: Evans E. H, De Lahunta A,  
619 editors. *Miller’s Anatomy of the Dog*. 4th ed. St. Louis, MO: Saunders; 2013, p.  
620 86–7.

621 [49] Schwarz T, Sullivan M, Hartung K. Radiographic anatomy of the cribiform plate  
622 (lamina cribrosa). *Vet Radiol Ultrasound* 2000;41:220–5.

623 [50] Sørgaard M, Linde JJ, Ismail H, Risum N, Kofoed KF, Kühl JT, Tittle B, Nielsen  
624 WB, Hove JD. Respiratory influence on left atrial volume calculation with 3D-  
625 echocardiography. *Cardiovasc Ultrasound* 2016;14:11.

626 [51] Riddervold F, Smiseth OA, Risoe C. The effect of positive end-expiratory  
627 pressure ventilation on atrial filling. *Acta Anaesthesiol Scand* 1991;35:448–52.

628 [52] Poutanen T. Left atrial volume assessed by transthoracic three dimensional  
629 echocardiography and magnetic resonance imaging: dynamic changes during  
630 the heart cycle in children. *Heart* 2000;83:537–42.

631 [53] Tidholm A, Bodegård-Westling A, Höglund K, Häggström J, Ljungvall I. Real-  
632 time 3-dimensional echocardiographic assessment of effective regurgitant  
633 orifice area in dogs with myxomatous mitral valve disease. *J Vet Intern Med*  
634 2017;31(2):303–10.

635 [54] Picker O, Scheeren TWL, Arndt JO. Inhalation anaesthetics increase heart rate  
636 by decreasing cardiac vagal activity in dogs. *Br J Anaesth* 2001;87:748–54.

1653  
1654  
1655  
1656  
1657  
1658  
1659  
1660  
1661  
1662  
1663  
1664  
1665  
1666  
1667  
1668  
1669  
1670  
1671  
1672  
1673  
1674  
1675  
1676  
1677  
1678  
1679  
1680  
1681  
1682  
1683  
1684  
1685  
1686  
1687  
1688  
1689  
1690  
1691  
1692  
1693  
1694  
1695  
1696  
1697  
1698  
1699  
1700  
1701  
1702  
1703  
1704  
1705  
1706  
1707  
1708  
1709  
1710  
1711

638 **Fig. 1**

639 Representative real-time biplane echocardiography images of the left atrium just  
640 before mitral valve opening corresponding to maximum left atrial volume (A and B) and  
641 left atrium just after mitral valve closure corresponding to minimum left atrial volume  
642 (C and D) were obtained. The endocardial borders were traced manually while  
643 excluding the left auricular appendage (\*) and the ostia of pulmonary veins, if visible.  
644 The mitral annulus was considered as the left atrioventricular border. The cut plane  
645 was adjusted from the left parasternal four-chamber view (A and C) in order to obtain  
646 a non-foreshortened two-chamber view (B and D).  
647 A: Left parasternal four-chamber view (0°) when left atrium is maximum. B: Left  
648 parasternal two-chamber view (90°) when left atrium is maximum. C: Left parasternal  
649 four-chamber view (0°) when left atrium is minimum. D: Left parasternal two-chamber  
650 view (90°) when left atrium is minimum.  
651 LA: left atrium; LV: left ventricle; RA: right atrium.

652 **Fig. 2**

653 Representative real-time three-dimensional echocardiography images of the left atrium  
654 in a dog. After automatic slicing of real-time three-dimensional echocardiography data  
655 set and manual alignment, manual input for placing reference points was carried out  
656 (one point at the dorsal border of the left atrium, one point at the hinge-point of the  
657 septal leaflet and one point at the hinge-point of the lateral leaflet). Following this step,  
658 automatic detection of endocardial surface in three dimensions was generated. In this  
659 example, manual adjustment by adding a total of 3 points in left apical four-chamber  
660 view (A), 3 points in left apical two-chamber view (B) and 5 points in left apical five-  
661 chamber view (C) was performed. These manual adjustments permitted accurate  
662 delineation of the left atrium cavity prior volume measurement by the software. Left



1712  
1713  
1714  
1715  
1716  
1717  
1718  
1719  
1720  
1721  
1722  
1723  
1724  
1725  
1726  
1727  
1728  
1729  
1730  
1731  
1732  
1733  
1734  
1735  
1736  
1737  
1738  
1739  
1740  
1741  
1742  
1743  
1744  
1745  
1746  
1747  
1748  
1749  
1750  
1751  
1752  
1753  
1754  
1755  
1756  
1757  
1758  
1759  
1760  
1761  
1762  
1763  
1764  
1765  
1766  
1767  
1768  
1769  
1770

663 atrial cast associated to the time-volume curve (E) were obtained. Notice the  
664 electrocardiographic tracing at the lower edge of the image correspond to the image  
665 just before mitral valve opening corresponding therefore to maximum left atrial volume.  
666 A: left apical four-chamber view. B: left apical two-chamber view. C: left apical five-  
667 chamber view. D: short axis view of the left atrium. Note that the plane can be adjusted  
668 through a perpendicular axis from the roof of left atrium to the mitral valve annulus. E:  
669 automatically reconstructed three-dimensional left atrial cavity cast and its  
670 corresponding typical time-volume curve (y axis indicates left atrial volume {mL}; x-axis  
671 indicates time {s}). ED: end atrial diastole corresponding to maximum left atrial volume;  
672 ES: end atrial systole corresponding to minimum left atrial volume

**Fig. 3**

673 Cardiac electrocardiographic-gated multi-detector computed tomography angiography  
674 in sagittal (A) and axial (E) planes. Regions of interest delineate the left atrium and  
675 extend from the dorsal border of the left atrium to the mitral valve annulus (B, C, D, F,  
676 G, H, J, K, L). Image I represents the computed three-dimensional volume.  
677 Ao: aorta; LA: left atrium; \*: left auricle; LV: left ventricle; RV: right ventricle.

**Fig. 4**

680 Correlations between real-time three-dimensional echocardiography (RT-3DE),  
681 biplane method of disk (MOD) and biplane area-length method (ALM) with the  
682 reference method multi-detector computed tomography angiography (MDCTA) for  
683 maximum left atrial volume (top) and minimum left atrial volume (bottom) of 20  
684 anesthetised dogs.  
685 When left atrial volume is maximal, there were a positive correlations between MDCTA  
686 and RT-3DE ( $r = 0.93$ ;  $p < 0.0001$ ) (A), MDCTA and biplane MOD ( $r = 0.81$ ;  $p < 0.0001$ )  
687 (C), and MDCTA and biplane ALM ( $r = 0.79$ ;  $p < 0.0001$ ) (E).

1771  
1772  
1773  
1774  
1775  
1776  
1777  
1778  
1779  
1780  
1781  
1782  
1783  
1784  
1785  
1786  
1787  
1788  
1789  
1790  
1791  
1792  
1793  
1794  
1795  
1796  
1797  
1798  
1799  
1800  
1801  
1802  
1803  
1804  
1805  
1806  
1807  
1808  
1809  
1810  
1811  
1812  
1813  
1814  
1815  
1816  
1817  
1818  
1819  
1820  
1821  
1822  
1823  
1824  
1825  
1826  
1827  
1828  
1829

688 Similarly, when left atrial volume is minimal, there were a positive correlations was  
689 detected when comparing MDCTA and RT-3DE ( $r = 0.82$ ;  $p < 0.0001$ ) (B), MDCTA and  
690 biplane MOD ( $r = 0.7$ ;  $p = 0.0006$ ) (D), and MDCTA and biplane ALM ( $r = 0.72$ ;  $p =$   
691  $0.0004$ ) (F).

692 Solid lines represent the coefficient of correlation; dashed lines represent the 95%  
693 confidence intervals.

694 Note that all methods correlate better for maximum left atrial volume.

695 ALM: area-length method;  $LAV_{max}$ : maximal left atrial volume;  $LAV_{min}$ : minimal left atrial  
696 volume; MDCTA: multi-detector computed tomography angiography; MOD: method of  
697 disk; RT-3DE: real-time three-dimensional echocardiography.

698 **Fig. 5**

699 Bland-Altman analysis showing the agreement between maximal (top) and minimal  
700 (bottom) left atrial volumes measured by the reference method, multi-detector  
701 computed tomography angiography, and those measured by real-time three-  
702 dimensional echocardiography (RT-3DE) (A and B), biplane method of disk (MOD) (C  
703 and D) or biplane area-length method (ALM) (E and F). Solid lines represent the mean  
704 difference (bias) and dashed lines represent the 95% limits of agreement ( $\pm 2$  SD from  
705 the mean between the two techniques used).

706 Note that MOD and ALM consistently overestimated left atrial volume, particularly at  
707 larger volume. By contrast, RT-3DE underestimated slightly left atrial volumes.

708 ALM: area-length method; MDCTA: multi-detector computed tomography  
709 angiography; MOD: method of disk; RT-3DE: real-time three-dimensional  
710 echocardiography; SD: standard deviation.

711

1830  
1831  
1832  
1833  
1834  
1835  
1836  
1837  
1838  
1839  
1840  
1841  
1842  
1843  
1844  
1845  
1846  
1847  
1848  
1849  
1850  
1851  
1852  
1853  
1854  
1855  
1856  
1857  
1858  
1859  
1860  
1861  
1862  
1863  
1864  
1865  
1866  
1867  
1868  
1869  
1870  
1871  
1872  
1873  
1874  
1875  
1876  
1877  
1878  
1879  
1880  
1881  
1882  
1883  
1884  
1885  
1886  
1887  
1888

712 **Table A** (supplementary data): Epidemiological and clinical characteristics of the 20  
713 dogs included in the study.

714 FE: female entire; FS: female spayed; MDCTA: multi-detector computed tomography  
715 angiography; ME: male entire; n.a: not available; NM: neutered male

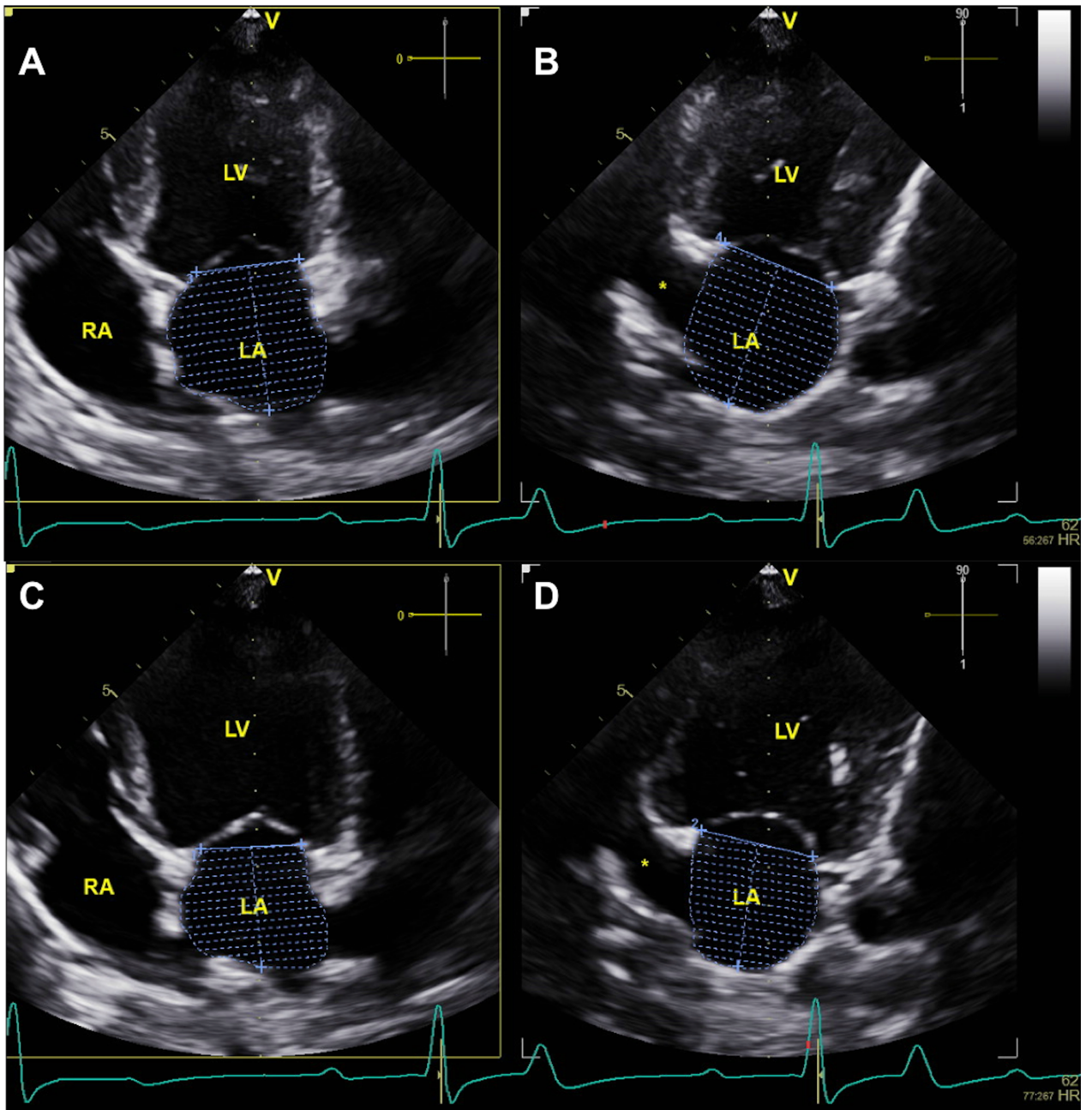
716 **Table 1:** Descriptive statistics of left atrial volume during maximum and minimum left  
717 atrial size. ALM: area-length method; LAV<sub>max</sub>: maximal left atrial volume; LAV<sub>min</sub>:  
718 minimal left atrial volume; MDCTA: multi-detector computed tomography  
719 angiography; MOD: method of disk; RT-3DE: real-time three-dimensional  
720 echocardiography.

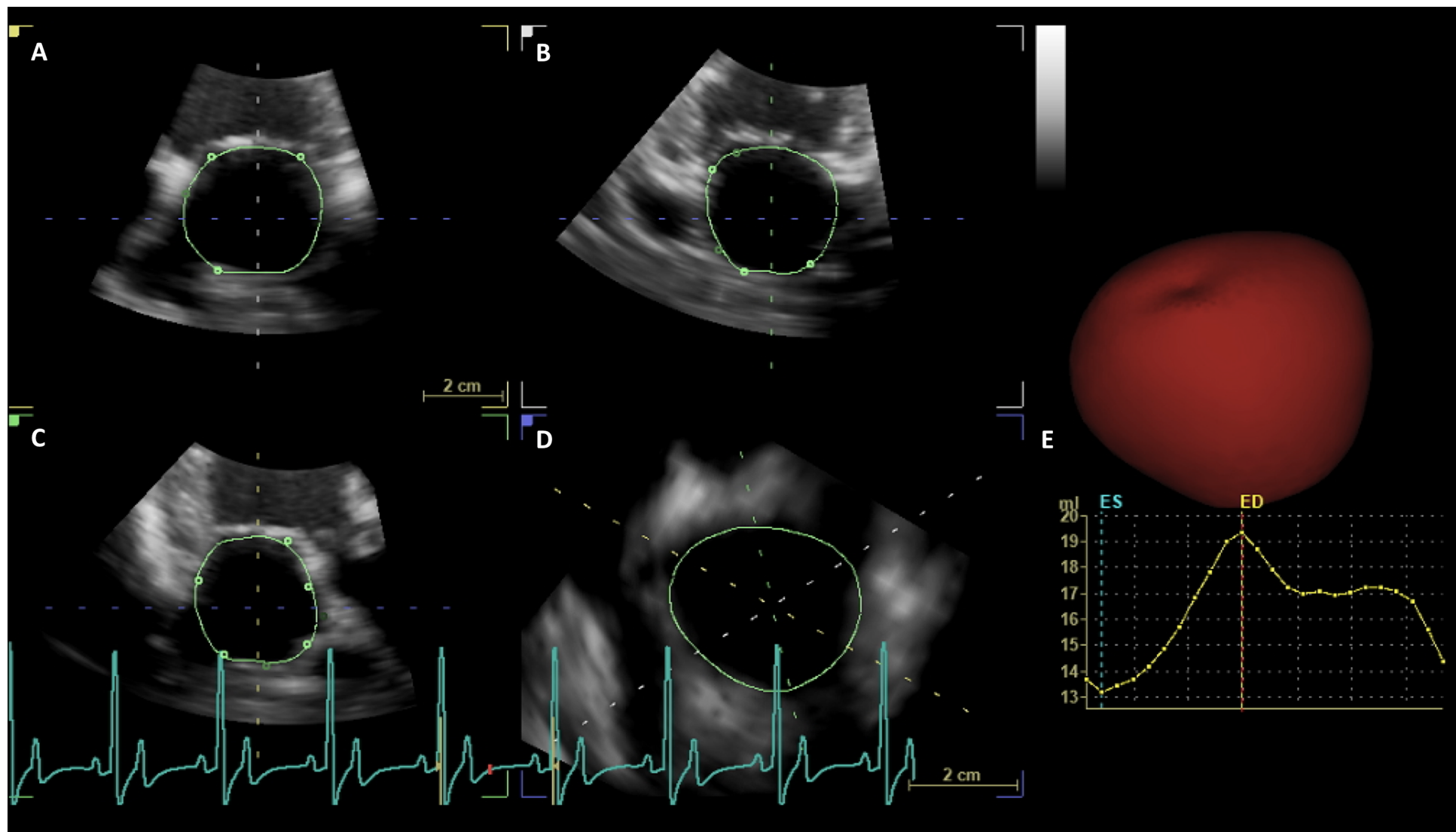
721 **Table 2:** Coefficient of variation for measurement of minimum left atrial volume and  
722 maximum left atrial volume according to different methods.

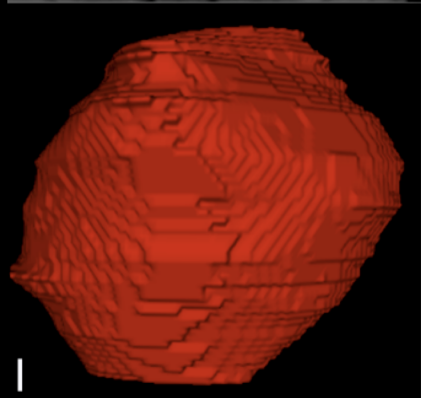
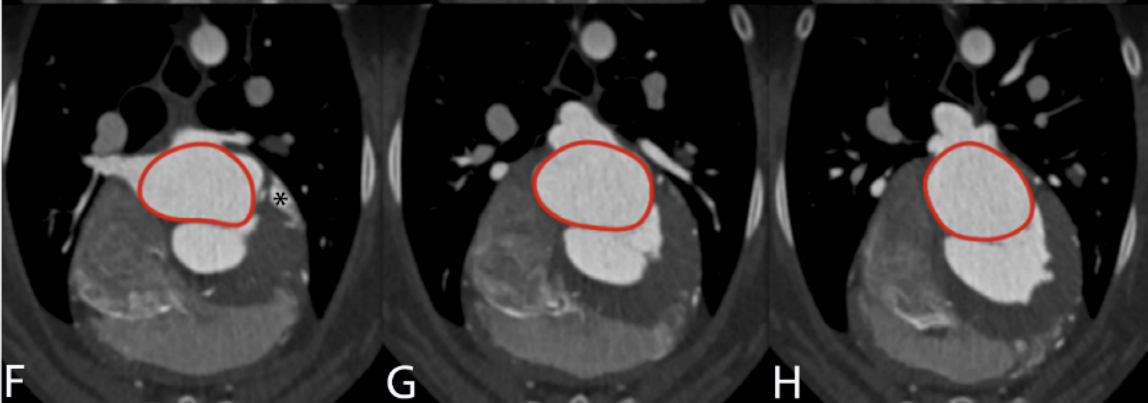
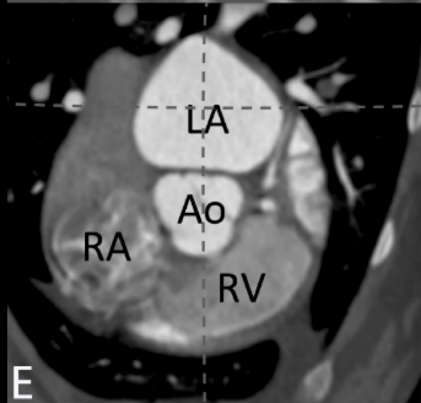
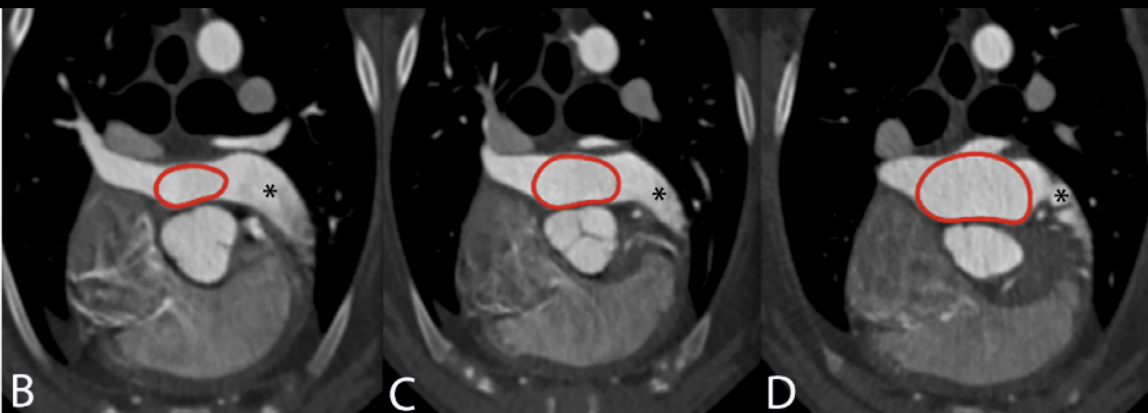
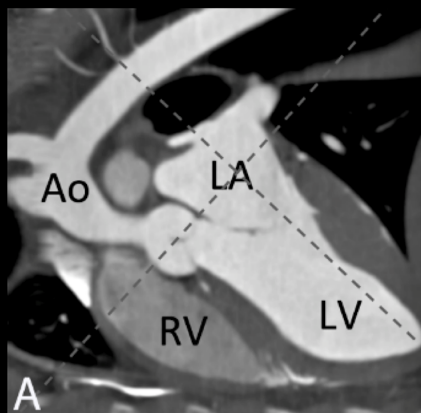
723 ALM: area-length method; CV: coefficient of variation; LAV<sub>max</sub>: maximal left atrial  
724 volume; LAV<sub>min</sub>: minimal left atrial volume; MDCTA: multi-detector computed  
725 tomography angiography; MOD: method of disk; RT-3DE: real-time three-  
726 dimensional echocardiography.

727 **Table 3:** Intraclass correlation coefficients and 95% CI reported for each part of  
728 measurements and for each parameter measured. Coefficient interpretation: 0 – 0.2  
729 indicates poor agreement; 0.3 – 0.4 indicates fair agreement; 0.5 – 0.7 indicates  
730 moderate agreement; 0.7 – 0.8 indicates strong agreement; and > 0.8 indicates almost  
731 perfect agreement.

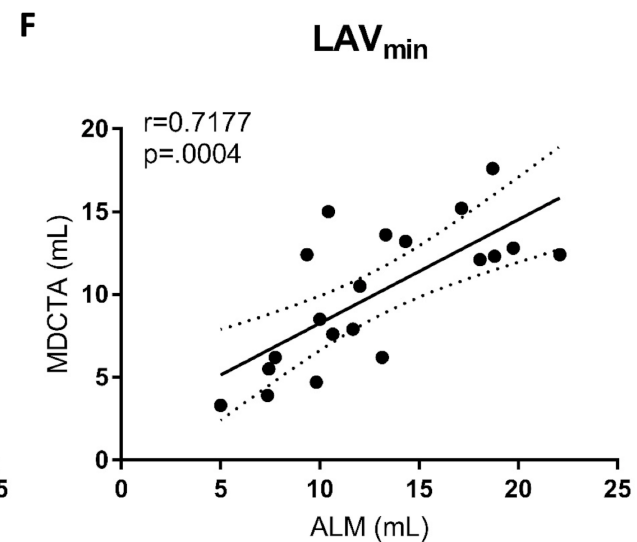
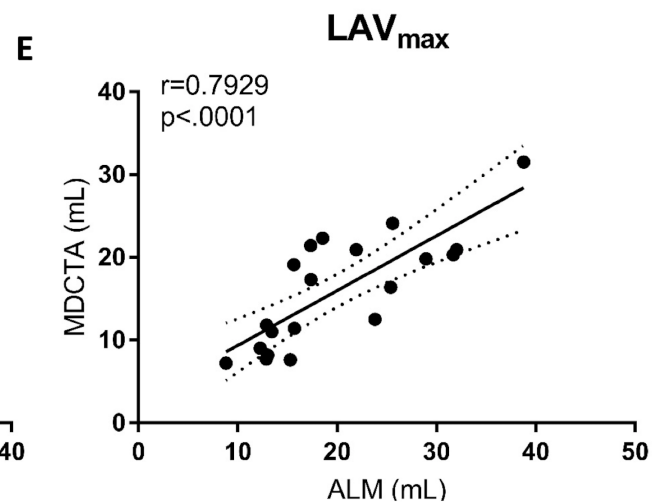
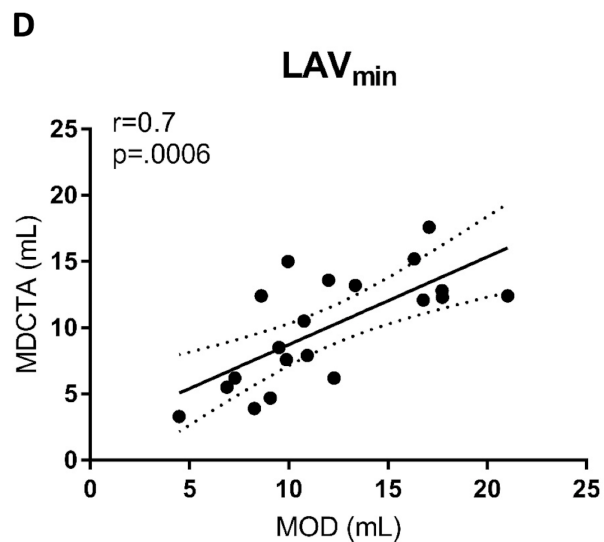
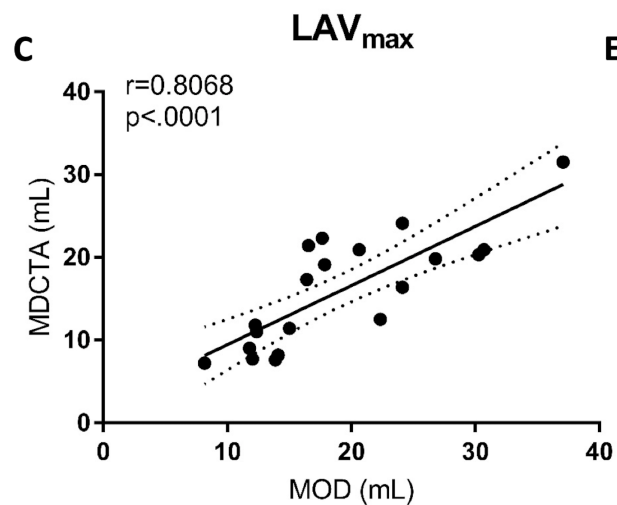
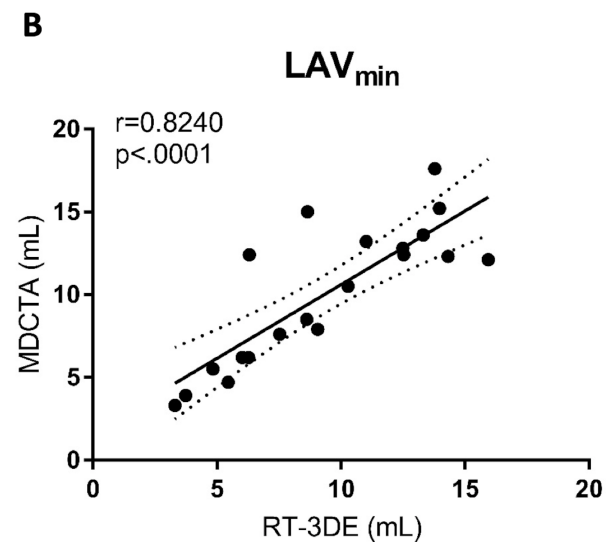
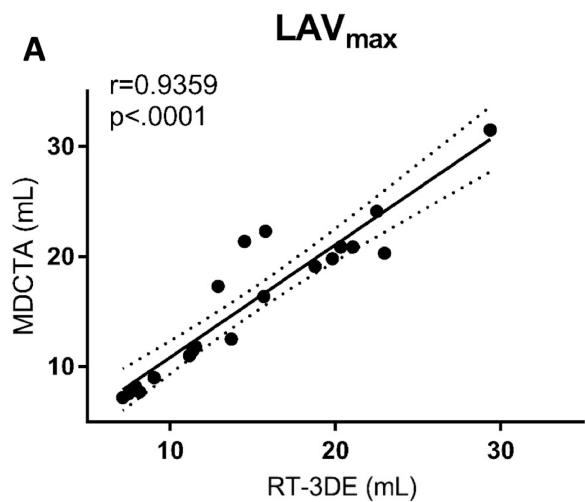
732 ALM: area-length method; CI: confidence interval; ICC: intraclass correlation; LAV<sub>max</sub>:  
733 maximal left atrial volume; LAV<sub>min</sub>: minimal left atrial volume; MDCTA: multi-detector  
734 computed tomography angiography; MOD: method of disk; RT-3DE: real-time three-  
735 dimensional echocardiography.

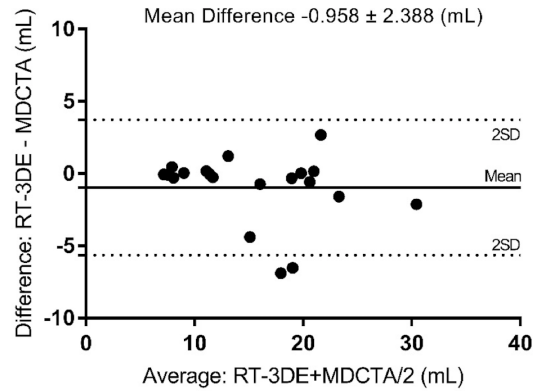
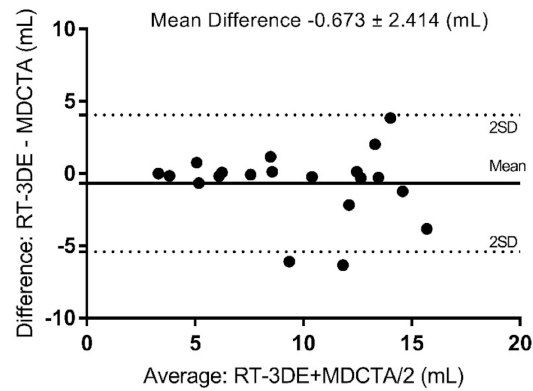
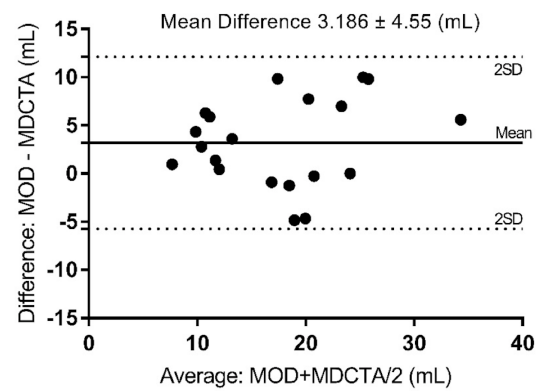
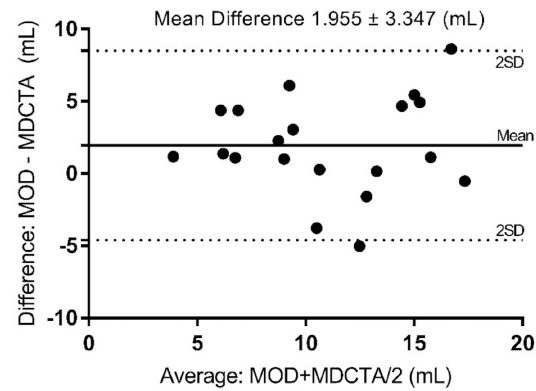
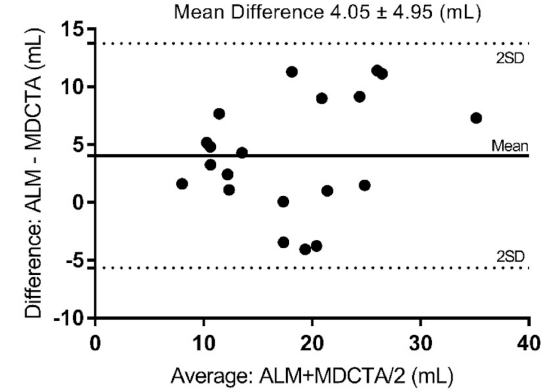
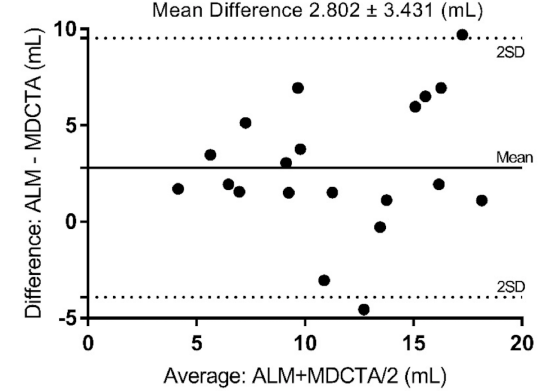










**A****Left atrial volume max: MDCTA vs RT-3DE****B****Left atrial volume min: MDCTA vs RT-3DE****C****Left atrial volume max: MDCTA vs MOD****D****Left atrial volume min: MDCTA vs MOD****E****Left atrial volume max: MDCTA vs ALM****F****Left atrial volume min: MDCTA vs ALM**



- 1 † Evans E. H, De Lahunta A. The Skeleton. In: Evans E. H, De Lahunta A,  
2 editors. Miller's Anatomy of the Dog. 4th ed. St. Louis, MO: Saunders; 2013, p.  
3 86–7.
- 4 ‡ Schwarz T, Sullivan M, Hartung K. Radiographic anatomy of the cribiform plate  
5 (lamina cribrosa). Vet Radiol Ultrasound 2000;41:220–5.

- 1 **Table A** (supplementary data): Epidemiological and clinical characteristics of the 20
- 2 dogs included in the study.
- 3 FE: female entire; FS: female spayed; MDCTA: multi-detector computed tomography
- 4 angiography; ME: male entire; n.a: not available; NM: neutered male

Dog	Breed	Sex	Age (days)	Body weight (kg)	Reason for MDCTA	Final diagnosis	Morphotype †‡
1	Cross breed	FS	1780	13	Cough	Chronic lower airway inflammation	mesaticephalic
2	Labrador Retriever	ME	268	28	Cough	Normal airway	mesaticephalic
3	Flat Coated Retriever	FE	2500	23.7	Nasal discharge	Aspergillosis	Mesati-Dolichocephalic
4	Cross breed	NM	1956	29.6	Nasal discharge	Aspergillosis	mesaticephalic
5	Golden Retriever	FS	3123	35.8	Cough	Bordetella Bronchiseptica	mesaticephalic
6	Schnauzer	ME	3617	14	Staging	Prostatic adenocarcinoma	n.a
7	Collie Rough	FS	4029	28.9	Staging	Mandible osteosarcoma	mesaticephalic
8	Golden Retriever	FE	4542	33.3	Exercise intolerance	Normal airway	n.a
9	Labrador Retriever	FS	3993	27.5	Staging	Oral malignant melanoma	Brachy-Mesaticephalic
10	Samoyed	FR	3493	27	Staging	Nasal transitional cell carcinoma	Brachy-Mesaticephalic
11	Cocker Spaniel	FS	747	10.7	Cervical mass	Neutrophilic pyogranulomatous inflammation	Mesati-Dolichocephalic

12	Golden Retriever	FR	222	18.85	exophthalmos	Retrobulbar abscess	mesaticephalic
13	Cross breed	ME	410	9.1	Cough	Tracheal collapse	mesaticephalic
14	Cross breed	NM	5218	25	Staging	Oral squamous cell carcinoma	mesaticephalic
15	Northern Inuit	NM	2324	44.5	Staging	Lymphoma	mesaticephalic
16	English Springer Spaniel	FS	3007	25.5	Sneezing	Nasal foreign body	mesaticephalic
17	Cocker Spaniel	NM	2502	14	Cough	Pulmonary foreign body	mesaticephalic
18	Border Collie	ME	2034	22.3	Nasal discharge	Rhinitis	mesaticephalic
19	Labrador Retriever	NM	4118	36	Cough	Bronchopneumonia	n.a
20	Boxer	NM	4542	30.3	Staging	Soft tissue sarcoma	brachycephalic

5

1 **Table 1:** Descriptive statistics of left atrial volume during maximum and minimum left  
2 atrial size. ALM: area-length method; LAV<sub>max</sub>: maximal left atrial volume; LAV<sub>min</sub>:  
3 minimal left atrial volume; MDCTA: multi-detector computed tomography  
4 angiography; MOD: method of disk; RT-3DE: real-time three-dimensional  
5 echocardiography.

Variable	Mean	Standard deviation	Minimum	Maximum
<b>LAV<sub>max</sub> (mL)</b>				
Biplane ALM	20.1	8.19	8.8	38.8
Biplane MOD	19.2	7.6	8.2	37.1
RT-3DE	15.1	6.2	7.1	29.4
MDCTA	16.0	6.7	7.2	31.5
<b>LAV<sub>min</sub> (mL)</b>				
Biplane ALM	12.9	4.8	5.0	22.1
Biplane MOD	12.0	4.4	4.5	21.0
RT-3DE	9.4	3.8	3.3	15.9
MDCTA	10.1	4.21	3.3	17.6
<b>LAV<sub>max</sub> (mL/kg)</b>				
Biplane ALM	0.63	0.31	0.29	1.43
Biplane MOD	0.68	0.34	0.32	1.55
RT-3DE	0.63	0.17	0.38	0.89
MDCTA	0.39	0.20	0.18	0.90
<b>LAV<sub>min</sub> (mL/kg)</b>				
Biplane ALM	0.35	0.18	0.17	0.81
Biplane MOD	0.40	0.20	0.19	0.91
RT-3DE	0.39	0.11	0.25	0.56
MDCTA	0.19	0.09	0.09	0.43



1 **Table 2:** Coefficient of variation for measurement of minimum left atrial volume and  
2 maximum left atrial volume according to different methods.  
3 ALM: area-length method; CV: coefficient of variation; LAV<sub>max</sub>: maximal left atrial  
4 volume; LAV<sub>min</sub>: minimal left atrial volume; MDCTA: multi-detector computed  
5 tomography angiography; MOD: method of disk; RT-3DE: real-time three-  
6 dimensional echocardiography.

	LAV <sub>min</sub> RT-3DE	LAV <sub>max</sub> RT-3DE	LAV <sub>min</sub> MOD	LAV <sub>max</sub> MOD	LAV <sub>min</sub> ALM	LAV <sub>max</sub> ALM	LAV <sub>min</sub> MDCTA	LAV <sub>max</sub> MDCTA
CV interobserver (%)	6.45	4.82	14.8	5.73	13.87	7.67	4.86	7.27
CV within day (%)	1.48	1.67	3.41	3.99	3.59	4.43	2.97	3.51
CV between day (%)	2.31	1.69	4.10	3.85	3.99	4.19	5.70	2.74

7

1 **Table 3:** Intraclass correlation coefficients and 95% CI reported for each part of  
 2 measurements and for each parameter measured. Coefficient interpretation: 0 – 0.2  
 3 indicates poor agreement; 0.3 – 0.4 indicates fair agreement; 0.5 – 0.7 indicates  
 4 moderate agreement; 0.7 – 0.8 indicates strong agreement; and > 0.8 indicates almost  
 5 perfect agreement.

6 ALM: area-length method; CI: confidence interval; ICC: intraclass correlation; LAV<sub>max</sub>:  
 7 maximal left atrial volume; LAV<sub>min</sub>: minimal left atrial volume; MDCTA: multi-detector  
 8 computed tomography angiography; MOD: method of disk; RT-3DE: real-time three-  
 9 dimensional echocardiography.

10

	LAV <sub>max</sub> MDCTA		LAV <sub>min</sub> MDCTA		
	ICC	95% CI		ICC	95% CI
LAV <sub>max</sub> RT-3DE	0.9322	0.8371 to 0.9726	LAV <sub>min</sub> RT-3DE	0.8215	0.6032 to 0.9253
LAV <sub>max</sub> ALM	0.7801	0.5244 to 0.9068	LAV <sub>min</sub> ALM	0.7109	0.4017 to 0.8746
LAV <sub>max</sub> MOD	0.8010	0.5635 to 0.9162	LAV <sub>min</sub> MOD	0.6989	0.3815 to 0.8689

11

# Journal of Veterinary Cardiology

The following information is required for submission:

## Author contribution

The ICMJE recommends that authorship be based on the following 4 criteria:

1. Substantial contributions to the conception or design of the work; or the acquisition, analysis, or interpretation of data for the work; AND
2. Drafting the work or revising it critically for important intellectual content; AND
3. Final approval of the version to be published; AND
4. Agreement to be accountable for all aspects of the work in ensuring that questions related to the accuracy or integrity of any part of the work are appropriately investigated and resolved.

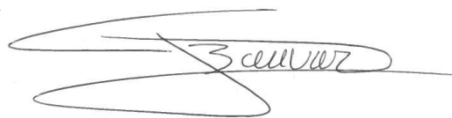
Please specify the contribution of **each author** to the paper, e.g. study concept or design, data collection, data analysis or interpretation, writing the paper, others, who have contributed in other ways, should be listed as contributors.

Yolanda Martinez Pereira, Florence Thierry, Geoff Culshaw, Tobias Schwarz and Ian Handel contributed substantially to the conception of the work and revising of the work and finally approving of the work and agree to accountable for all aspects of the work

As **Corresponding Author** I hereby confirm that all listed authors in the submission meet these Criteria.

Corresponding author: Jonathan Bouvard

Please add signature here:



Date: 09/11/2018